

Probing Strangeness in Hard Processes

The science case of a RICH detector for CLAS12

H. Avakian⁷, M. Battaglieri⁵, E. Cisbani⁶, M. Contalbrigo³, U. D'Alesio², R. De Leo¹, R. Devita⁵,
P. Di Nezza⁴, D. Hasch⁴, V. Kubarovsky⁷, M. Mirazita⁴, M. Osipenko⁵, L. Pappalardo³, P. Rossi⁴

¹Istituto Nazionale di Fisica Nucleare, Sezione di Bari and University of Bari, Bari, Italy

²Istituto Nazionale di Fisica Nucleare, Sezione di Cagliari and University of Cagliari, Cagliari, Italy

³Istituto Nazionale di Fisica Nucleare, Sezione di Ferrara, Ferrara, Italy

⁴Istituto Nazionale di Fisica Nucleare, Laboratori Nazionali di Frascati, Frascati, Italy

⁵Istituto Nazionale di Fisica Nucleare, Sezione di Genova, Genova, Italy

⁶Istituto Nazionale di Fisica Nucleare, Sezione di Roma, and Istituto Superiore di Sanita Roma, Italy

⁷Thomas Jefferson National Accelerator Facility, Newport News, VA, USA

November 6, 2018

Abstract

Since the discovery of strangeness almost five decades ago, interest in this degree of freedom has grown up and now its investigation spans the scales from quarks to nuclei. Measurements with identified strange hadrons can provide important information on several hot topics in hadronic physics: the strange distribution and fragmentation functions, the nucleon tomography and quark orbital momentum, accessible through the study of the *generalized* parton distribution and the *transverse momentum dependent* parton distribution functions, the quark hadronization in the nuclear medium, the hadron spectroscopy and the search for exotic mesons.

The CLAS12 large acceptance spectrometer in Hall B at the Jefferson Laboratory upgraded with a RICH detector together with the 12 GeV CEBAF high intensity, high polarized electron beam can open new possibilities to study strangeness in hard processes allowing breakthroughs in all those areas.

This paper summarizes the physics case for a RICH detector for CLAS12. Many topics have been intensively discussed at the International Workshop "Probing Strangeness in Hard Processes" (PSHP2010) [1] held in Frascati, Italy in October 2010. The authors of this papers like to thank all speakers and participants of the workshop for their contribution and very fruitful discussion.

Contents

1	Executive Summary	3
1.1	Nucleon structure and the role of strangeness	3
1.2	Effects of the nuclear medium	4
1.3	Search for exotic mesons	4
1.4	Impact of CLAS12 with a RICH	5
2	The Longitudinal Structure of the Nucleon	6
2.1	Semi-inclusive DIS - a brief Introduction	6
2.2	Open issues for quark distributions at medium and high x	7
2.2.1	Strangeness momentum distribution	7
2.2.2	Strangeness helicity distribution	9
2.3	Fragmentation functions	10
3	The Transverse Structure of the Nucleon	13
3.1	Introduction	13
3.2	Spin and azimuthal asymmetries in semi-inclusive DIS	15
3.2.1	The kaon “puzzle”	16
3.2.2	Hunting for the Collins function for kaons	18
3.2.3	Dihadron production in semi-inclusive DIS and transversity	19
3.3	Spin and azimuthal asymmetries in pp collisions	20
4	Nucleon Imaging: GPDs and Exclusive Processes	22
4.1	Introduction	22
4.2	Hard exclusive meson production	22
4.2.1	Exclusive ϕ -meson production	23
5	Hadronization in the Nuclear Medium	25
5.1	Introduction	25
5.2	SIDIS and hadronization in cold nuclear matter	25
5.2.1	Nuclear attenuation	25
5.2.2	Medium modification of the transverse momentum	26
5.2.3	Medium modification of TMD distributions	27
6	Spectroscopy: Hidden Strangeness and Strangeonia	29
6.1	Hybrids with hidden strangeness	29
6.2	Strangeonia	30
7	Acknowledgement	32

1 Executive Summary

1.1 Nucleon structure and the role of strangeness

Lepton scattering is the basic tool for determining the fundamental structure of matter, in particular of the nucleon, from which the observable physical world around us is formed. Such experiments, using high energy electron beams, tested successfully the theory of Quantum Chromodynamics (QCD), which describes all strongly interacting matter in terms of quark and gluon degrees of freedom. The successful prediction of the energy dependence of parton distributions, which were introduced to describe the structure of the nucleon, has been one of the great triumphs of perturbative QCD.

After four decades of lepton-nucleon scattering experiments, the gain in precision has often revealed intriguing aspects of the nucleon structure. Among these surprises are the sizeable breaking of isospin symmetry in the light sea quark sector, suggesting differences between the sea quark and antiquark distributions, the steep rise of the distributions at small momentum fractions, and an interesting pattern of modifications of the distributions in nuclei. Certainly one of the most surprising results is the unexpectedly small fraction, about a quarter, of the proton's spin that is due to the contribution from quarks and antiquarks. This finding has triggered a vast experimental and theoretical activity aiming at clarifying the role gluons and parton orbital angular momenta play for a complete description of the proton spin structure. New concepts of Transverse Momentum Dependent (TMD) distribution and fragmentation functions, which go beyond the collinear approximation, are a key to unravel the intricacies of the intrinsic motion of partons and the possible connection between their orbital motion, their spin and the spin of the nucleon, which cannot be described with standard (e.g. collinear) parton distributions. These TMD distributions together with the so-called Generalized Parton Distributions (GPDs) provide for the first time a framework to obtain information towards a genuine multi-dimensional momentum and space resolution of the nucleon structure. This knowledge will have an important impact to other fields. Giving just one example, the information about the initial spatial distribution of quarks and gluons in the nucleon is essential for the interpretation of heavy-ion collision data and the quest for the Quark-Gluon-Plasma. The mapping of GPDs and TMDs and the deduction of a three-dimensional image of the nucleon is a major focus of the hadron physics community and constitutes a milestone in the physics program of the Jefferson Laboratory (JLab) 12 GeV upgrade¹ [2].

While GPDs can be probed in hard exclusive processes observed in high energy lepton-nucleon scattering, TMDs are most successfully measured in semi-inclusive deep-inelastic scattering (SIDIS). In SIDIS experiments, also a hadron is detected in the final state in addition to the scattered lepton. These experiments are the most powerful tool for directly obtaining flavour dependent information about the nucleon's quark structure. In particular, they provide unique access to the elusive strange distributions. Pioneering polarized semi-inclusive DIS experiments have revealed surprising effects in various different kaon production observables, which deviate from the expectations based on u -quark dominance for the scattering off a proton target. These kaon results point to a significant role of sea quarks, and in particular strange quarks. For almost all kaon observables, the deviation from the expected behaviour is most pronounced in the kinematic region around $x_B = 0.1$ (x_B being the Bjorken scaling variable), which is well covered by CLAS12. In order to fully explore the power of SIDIS experiments, pion, kaon and proton separation over the full accessible kinematic range is essential.

¹With the JLab 12 GeV upgrade, up to 11 GeV electron beams will be delivered to Hall A, B and C and a 12 GeV electron beam to Hall D.

With the 12 GeV upgrade, JLab will provide the unique combination of high beam energy, high intensity (luminosity) and polarization, the usage of polarized targets and advanced detection capabilities necessary for a mapping of the novel TMDs and GPDs. These functions will be uniquely explored in the valence kinematic region where many new, intriguing aspects of nucleon structure are expected to be most relevant. The addition of a RICH detector to the CLAS12 large acceptance spectrometer would make the upgraded Hall B an ideal place for carrying out these studies and shading light on the elusive strange distribution and on the role sea quarks may play in a complete, three-dimensional description of nucleon structure.

1.2 Effects of the nuclear medium

Besides the exciting new aspects of nucleon structure, a very interesting pattern of modifications of parton distribution and fragmentation functions in nuclei has been observed, which caused vast experimental and theoretical activities. The understanding of quark propagation in the nuclear medium is crucial for the interpretation of high energy proton-nucleus interactions and ultrarelativistic heavy-ion collisions. Leptonproduction of hadrons has the virtue that the energy and momentum transferred to the hit parton are well determined, as it is “tagged” by the scattered lepton and the nucleus is basically used as a probe at the fermi scale with increasing size or density, thus acting as femtometer-scale detectors of the hadronization process. Theoretical models can therefore be calibrated in nuclear semi-inclusive DIS and then applied, for example, to studies of the Quark-Gluon-Plasma.

The experimental results achieved over the last decade, demonstrate the enormous potential of nuclear SIDIS in shading light on the hadronization mechanisms. For all observables investigated so far, a very distinct pattern of nuclear effects was observed for the various different hadron types. However, the existence and relative importance of the various stages, like the propagation and the interaction of the partons, color-neutralization and formation of the final hadron, are far from being determined unambiguously.

In this panorama, JLab12 with its high beam intensity and the usage of a large variety of nuclear targets will provide data in a kinematic region that is very suitable for studies of nuclear effects. The potential of performing a fully differential analysis is a key to disentangle the various different stages of hadronization. The capability of identifying pions, kaons and protons over the whole kinematic range of interest is essential for gaining more insights into the space-time evolution of the hadronization process.

1.3 Search for exotic mesons

The phenomenology of hadrons and in particular the study of their spectrum led more than forty years ago to the development of the quark model, where baryons and mesons are described as bound systems of three quarks and of a quark-antiquark pair, respectively. Beyond these experimentally extensively observed states, phenomenological models and lattice QCD calculations suggest also the existence of exotic configurations such as hybrids (qqg), tetraquarks ($qq\bar{q}\bar{q}$) and glueballs. The experimental verification of such exotic states would significantly deepen our knowledge about the dynamics of QCD. A very attractive method to identify exotic mesons is through strangeness-rich final states, where the kaons from the decay of the involved ϕ -meson are usually high energetic. Kaon identification over the whole accessible momentum range would hence provide unique capabilities for the study of strangeonia and the search for exotic mesons.

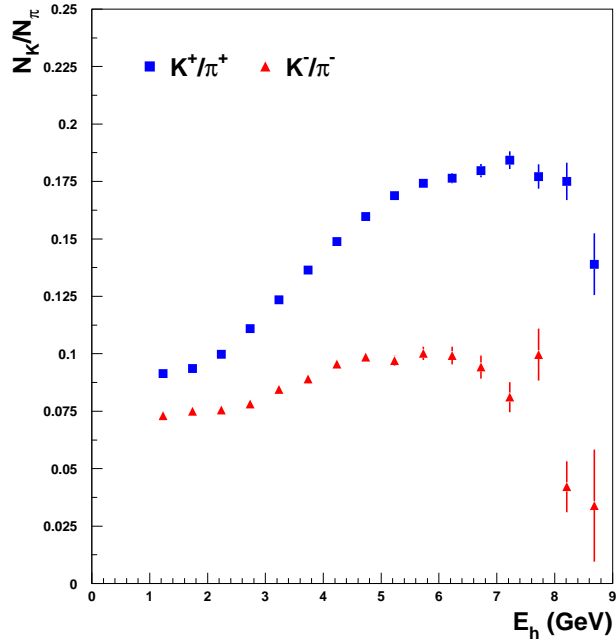


Figure 1: The ratio of semi-inclusively produced kaons and pions as function of the kaon energy using a Monte Carlo simulation with 11 GeV electron beam. The requirement on fractional hadron momentum $z_h > 0.2$ is applied.

1.4 Impact of CLAS12 with a RICH

The exciting physics program for CLAS12 is based on the unique features of the upgraded CEBAF and CLAS12 spectrometer:

- high beam energy and intensity,
- high beam polarization,
- longitudinally and transversely polarized proton and effective neutron targets,
- variety of nuclear targets,
- large acceptance, multipurpose spectrometer.

The addition of a RICH detector would significantly enhance the particle identification capabilities of CLAS12 and make Hall B a unique place for studying the physics topics summarized above. Figure 1 presents the ratio of semi-inclusively produced kaons and pions as function of the kaon energy using a Monte Carlo simulation with 11 GeV electron beam. The obtained distribution shows that kaon identification up to 8 GeV is highly desirable in order to fully explore the power of SIDIS experiments. Furthermore, as pions greatly outnumber the other hadrons at nearly all kinematics, the RICH detector can tremendously reduce the backgrounds for the detection of unstable particles that decay to at least one charged non-pion.

2 The Longitudinal Structure of the Nucleon

2.1 Semi-inclusive DIS - a brief Introduction

The exploration of the internal structure of hadrons in terms of quarks and gluons, the fundamental degrees of freedom of QCD, has been and still is at the frontier of hadronic high energy physics. Experiments with inclusive Deep-Inelastic Scattering (DIS) processes, $\ell N \rightarrow \ell' X$, have been performed for decades and have been interpreted as the most common way to investigate the internal structure of nucleons (protons and neutrons). Within the standard framework of leading-twist perturbative QCD (pQCD) and its collinear factorization theorems, the cross section for this inclusive process, at large momentum transfer Q^2 , can be expressed as a convolution of parton distribution functions (PDF), $f_{a/p}(x)$, giving the number density of partons, a , with a certain fraction x of the momentum of the parent hadron, p , with calculable elementary hard interactions. The successful prediction of the scale (Q^2) dependence of PDFs has been one of the great triumphs of pQCD.

A further and crucial insight in the internal structure of the nucleon can be obtained by exploring its spin content. The helicity distributions

$$\Delta f_{a/N} = f_{+/+} - f_{-/+}, \quad (1)$$

where $f_{\pm/+}$ is the probability of finding a parton with helicity \pm in a nucleon with positive helicity, can be studied in polarized DIS processes where both beam lepton and target nucleon are longitudinally polarized.

Although very successful, inclusive DIS offers only limited information about the internal nucleon structure and does not allow for a direct flavour decomposition or an access to transverse degrees of freedom. A major and leading role in such efforts is played by Semi-Inclusive Deep-Inelastic Scattering (SIDIS) processes, $\ell N \rightarrow \ell' h X$, where in addition to the scattered lepton, also a hadron is detected in the final state. This hadron is generated in the fragmentation of the scattered quark – the so-called current fragmentation region. For such processes the pQCD factorization theorem implies the following expression:

$$\frac{d\sigma^{\ell p \rightarrow \ell' h X}}{dx_B dz_h dQ^2} = \sum_q f_{a/p}(x, Q^2) \otimes d\hat{\sigma}^{\ell a \rightarrow \ell' c} \otimes D_{h/c}(z_h, Q^2), \quad (2)$$

where

$$x_B = \frac{Q^2}{2p \cdot q} \quad z_h = \frac{p \cdot P_h}{p \cdot q} \quad Q^2 = -(l - l')^2. \quad (3)$$

Here, l, l', p and q are, respectively, the four-momenta of the incoming and scattered lepton, the target nucleon and the exchanged virtual boson. In Eq. (2) besides the PDF $f_{a/p}$, discussed above, a new quantity, related to the hadronization of the scattered quark appears: the fragmentation function (FF) $D_{h/c}(z_h)$, giving the probability for a parton c to produce a hadron h with a fraction z_h of the momentum of the struck quark.

By studying a specific final hadron one can properly “weight” the flavour of the incoming quark in the parent hadron and achieve a more clear picture of the internal proton structure. Analogously, polarized semi-inclusive DIS processes help for a much deeper exploration towards a flavour decomposition of the longitudinal spin content of the nucleon.

Both parton distribution and fragmentation functions cannot be calculated in pQCD which, however, predicts their scale dependence. This remarkable feature of pQCD together with the universality property of these functions, allows for their extraction from a suitable hard scattering

process and their usage in phenomenological studies of any hard scattering process. Famous examples are the calculation of inclusive hadron production in hadron-hadron collisions, $pp \rightarrow hX$, or in e^+e^- annihilation processes where only fragmentation functions enter the latter; or dilepton production in hadron-hadron collision (Drell-Yan processes), which involves only distribution functions. A more efficient strategy, still based on the universality of distribution and fragmentation functions, is the approach of performing global fits by combining simultaneously data from different processes and at different scales.

While leading order (LO) calculations simply extend the parton model expressions by including proper pQCD scale dependence, higher order computations in the strong coupling constant, and in particular next-to-leading order (NLO) calculations, explored and validated for most processes, provide access to parton distributions for the various quark flavours and the gluon even from fully inclusive processes due to the different scaling behaviour of individual quarks and the gluon. NLO global analyses have become a very powerful tool for determining PDFs and FFs provided the availability of data sets over a wide kinematic range and, preferably, from various different processes. In fact, the complementary information on the various partons obtained by combining measurements from different processes allows to relax and test rather stringent assumptions on the parameterizations adopted in the QCD fits and to probe the extracted functions in various different energy regimes and kinematic configurations.

2.2 Open issues for quark distributions at medium and high x

Modern global analyses of parton distribution and fragmentation functions use data from a large variety of different processes in order to determine as much as possible different aspects of these functions (for a recent review see for example [3]). With the availability of HERA – a QCD machine – impressive progress was made over the last two decades in extracting parton distributions.

However, certain components even of the collinear structure of the nucleon are still poorly determined. Foremost among these is the elusive strangeness distribution. But also the behaviour of parton distributions for $x \rightarrow 1$ is still under debate due to the lack of precise data in the very high x region.

2.2.1 Strangeness momentum distribution

The determination of strangeness is challenging as it has the same electroweak couplings as the down distribution while it is typically much smaller than it. In absence of significant experimental constraints, the lack of knowledge is reflected in the common practice of adopting the simplified ansatz $\bar{s} = s = C_s/2(\bar{u} + \bar{d})$, where even the proportionality constant C_s is only very loosely constrained by data. The only way of determining the strange distribution accurately from data is to include semi-inclusive information. Useful but limited information is provided by neutrino and antineutrino charm production (known as dimuon production) which is sensitive to strange distributions through the LO partonic process $W^+ + s \rightarrow c$. The limitations in constraining the two strange combinations $s^+ = s + \bar{s}$ and $s^- = s - \bar{s}$ are illustrated in Fig. 2 and Fig. 3 showing extractions of the strange distributions by the CTEQ-group and the NNPDF-group, respectively. All shown extractions also include the information from the neutrino dimuon data. In Fig. 2, the solid (red) curve shows the reference PDF set CTEQ6.5S0. The other curves illustrate the range of variation of the magnitude and shape of $s^\pm(x)$ that are consistent with the data used in the fits [4].

Figure 3 (left) also shows the result for s^- obtained when assuming the strange distribution being proportional to the light quark sea, i.e. $\bar{s} = s = C_s/2(\bar{u} + \bar{d})$. This result is then misleadingly

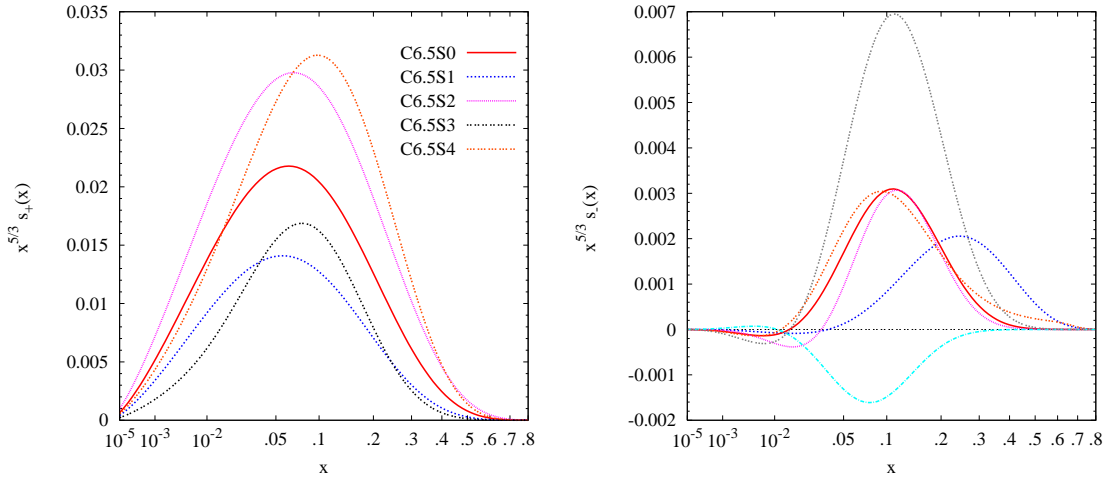


Figure 2: Variations of the strange distributions $s^+ = s + \bar{s}$ (left) and $s^- = s - \bar{s}$ (right) for the five PDF sets CTEQ6.5Si, $i = 0, \dots, 4$ [4] that are consistent with the data used in the fits.

accurate as demonstrated by the full (red) line (NNPDF1.0). Very recently, the NNPDF-group derived a new, by a factor of two in the uncertainty improved, strange distribution by comparing Drell-Yan cross section data above and below the charm threshold [5] (labelled as NNPDF2.0 or NNPDF2.1 in Fig. 3). The most recent NNPDF extraction of $s^- = s - \bar{s}$ (NNPDF2.1 [6]) is compared in Fig. 3 (right) with those from the CTEQ (CT10 [7]) and MSTW (MSTW08 [8]) groups. Here, the NNPDF strangeness distribution is parameterized with as many parameters as any other PDF resulting an uncertainty that is mostly larger than the one of MSTW08 and CT10 strangeness sets, which use very few parameters. Clearly, much more data is needed for pinning down the strangeness distribution.

Complementary and new information about the strange content of the nucleon is provided by kaon electroproduction data from semi-inclusive DIS. The high potential of information contained in such data has been illustrated by the HERMES collaboration which performed a LO extraction of the strange distribution $S = s^+ = s + \bar{s}$ from charged-kaon production in DIS on the deuteron [9], shown in Fig. 4. This result confirms that the strange distribution is substantially different from the average of the light sea quarks.

Such data from charged kaon production in DIS were already successfully included in NLO global QCD analyses of helicity distributions where they provide stringent constraints for a flavour separation, as discussed in the next section. Their inclusion in global QCD analyses of momentum distributions is still an open but promising task, in particular in view of new SIDIS data which will be available in near future from COMPASS and CLAS12 experiments. As seen in Fig. 4, the deviation of the strangeness distribution from the expected behaviour is most pronounced in the kinematic range around $x = 0.1$ which is well covered by CLAS12. Kaon identification over the whole momentum range will be an essential ingredient for shading light on the elusive strange distribution.

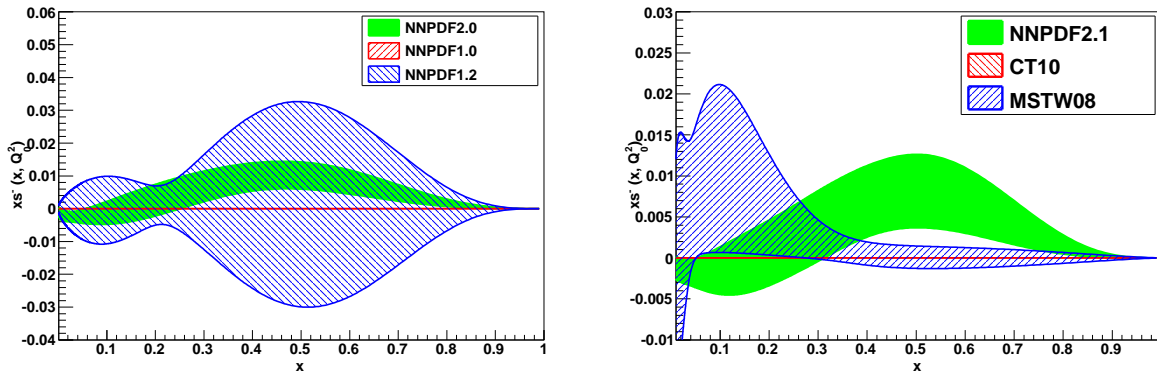


Figure 3: The strange distribution $s^- = s - \bar{s}$. Left: the NNPDF extraction [5] of xs^- determined in a fit to DIS including dimuon data (NNPDF2.0) and not including them (NNPDF1.2). A fit without dimuon data where the strange distribution is fixed by the assumption $\bar{s} = s = C_s/2(\bar{u} + \bar{d})$ with $C_s = 0.5$ (NNPDF1.0) is also shown by the full (red) line. Right: most recent NNPDF extraction of xs^- (NNPDF2.1 [6]) compared with extractions from the CTEQ (CT10 [7]) and MSTW (MSTW08 [8]) groups.

2.2.2 Strangeness helicity distribution

Modern global QCD analyses of helicity parton distributions make use of data from both inclusive and semi-inclusive polarized DIS, as well as from polarized proton-proton (pp) scattering at RHIC. In absence of inclusive *polarized* DIS data from a *collider*, sea quark and gluon helicity distributions can only be poorly constrained from scaling violation. Therefore, from the early days of analyses of polarized data, there was an attempt to use data that provide more direct flavour information and/or access to the gluon polarization. But only recently, a comprehensive, fully NLO QCD analysis of available polarized data, including pp scattering data, has been developed by the DSSV-group [13, 14]. This analysis benefited significantly from the improved knowledge

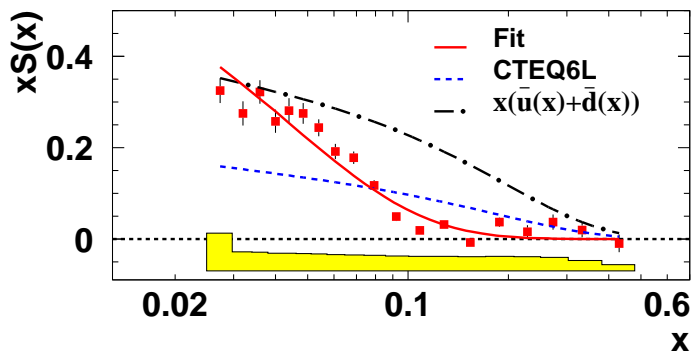


Figure 4: The strange distributions $S = s^+ = s + \bar{s}$ extracted in a LO analysis by the HERMES experiment [9] using data from SIDIS kaon production. The solid curve is a 3-parameter fit for $S(x) = x^a e^{-x/b}(1-x)$ and the dot-dashed curve is the sum of light antiquarks from CTEQ6L. The shape of S is found to be very different from the average of the light sea.

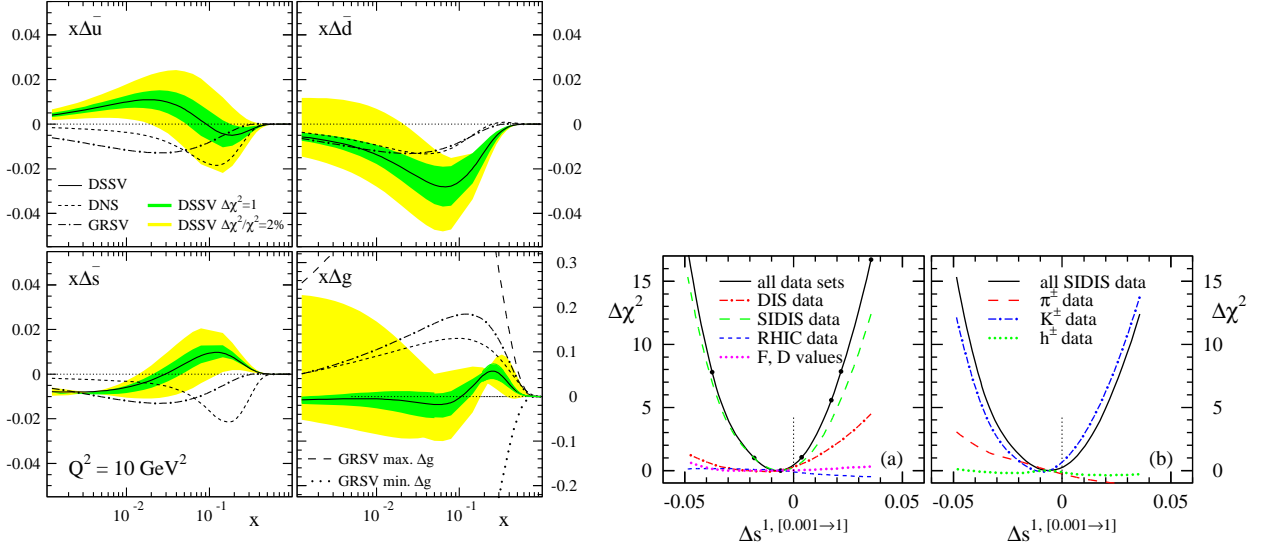


Figure 5: Left: DSSV polarized sea and gluon densities compared with previous fits [10, 11, 12]. The shaded bands correspond to alternative fits with uncertainties $\Delta\chi^2 = 1$ and $\Delta\chi^2/\chi^2 = 2\%$. Right: the χ^2 profiles and partial contributions $\Delta\chi^2$ of the various types of data sets for variations of the truncated first moment Δs^1 for the range $0.001 < x < 1.0$.

of parton-to-hadron fragmentation functions derived by the DSS-group [15]. For the first time, these fragmentation functions provide a good description of identified hadron yields in the entire kinematic range relevant for the analysis of polarized semi-inclusive DIS and pp scattering data.

While the up and down quark helicity distributions could be determined with rather good precision in the range $0.001 < x < 0.8$ already by earlier global analyses, the sea quark and gluon polarization could only, still poorly, be constrained with the inclusion of information from SIDIS and pp scattering data, as shown in Fig. 5 (left panels).

The impact of SIDIS data is greatly illustrated with the extraction of the strange quark polarization. Figure 5 (right) shows the χ^2 profiles for the partial contributions ($\Delta\chi^2$) of the various types of data sets, which clearly demonstrates that the information from SIDIS kaon production provides the most stringent constraints on the shape of the strange helicity distribution. The newly derived strange polarization is consistent with recent results from HERMES [9] and COMPASS [16] experiments, but exhibits a shape that is very different from those distributions obtained in earlier global NLO extractions, which employed constraints based on the assumption of SU(3) symmetry. The polarization of strange quarks has been a focus since the very beginning of the 'proton spin crises' and our poor knowledge so far emphasizes the need for much more precise data of semi-inclusive kaon production over a wide kinematic range.

2.3 Fragmentation functions

Very precise and clean information on parton-to-hadron fragmentation functions is provided by data from electron-positron annihilation into charged hadrons. Such data, however, do not allow to disentangle quark from antiquark fragmentation without employing model dependent so-called

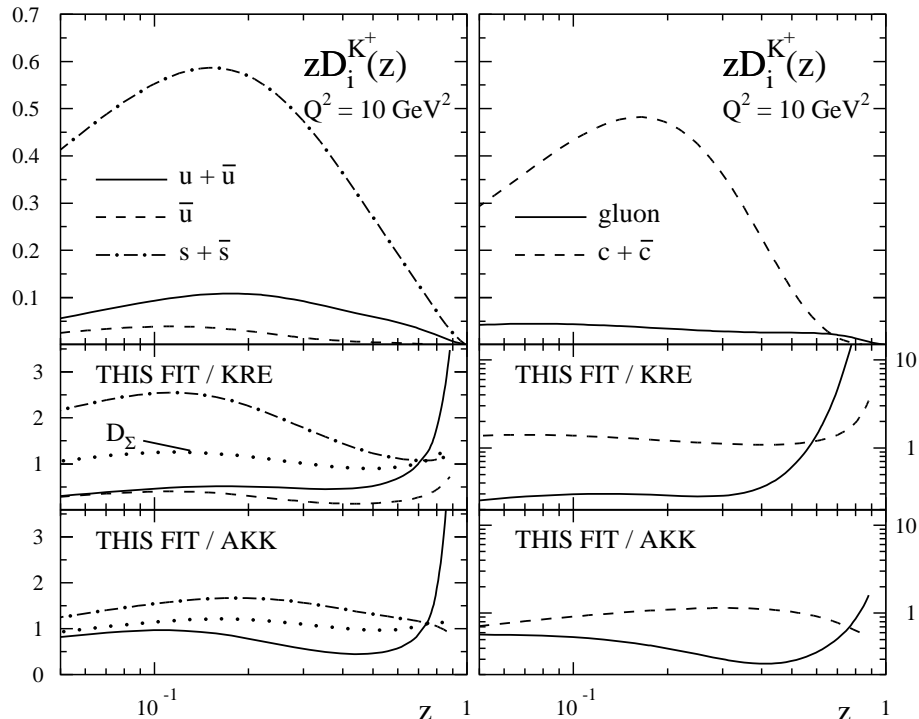


Figure 6: Upper panels: the DSS individual fragmentation functions for positively charged kaons $zD_i^{K^+}$ for $i = u + \bar{u}$, \bar{u} , $s + \bar{s}$, g , and $c + \bar{c}$. Middle panels: ratios of DSS fragmentation functions to the ones of KRE [18]. The dotted line indicates the ratio for singlet combination of fragmentation functions $zD_\Sigma^{K^+}$, where Σ represents the sum over all quark flavours. Lower panels: ratios of DSS fragmentation functions to the ones of AKK [19]; note that $D_{\bar{u}}^{K^+}$ is not available in the AKK analysis.

'tagging' techniques. Also gluon fragmentation is only poorly determined because of lack of precise enough data at energy scales away from the Z -resonance. As for PDFs, complementary information on the flavour dependence of the fragmentation process can be obtained from single-hadron production in pp collisions and semi-inclusive DIS. These new data together with very precise PDF-sets allow for direct flavour tagging of fragmentation functions.

Such a comprehensive global QCD analysis was performed by the DSS-group [15, 17]. For the first time, these new pion and kaon fragmentation functions reproduce well the wealth of precise electron-positron annihilation data *and* electron-proton and proton-proton observables. Figure 6 shows the DSS individual quark fragmentation functions for K^+ and compares the new set with earlier extractions by KRE [18] and AKK [19] based only on e^+e^- annihilation data and *assumptions* for a flavour separation. The new fragmentation functions are very distinct from the earlier ones in emphasizing the role of strangeness in kaon production (but also in pion production, see Ref. [17]). This result is driven by the charged kaon data measured in semi-inclusive DIS by the HERMES experiment and in pp scattering by the BRAHMS experiment. In particular the SIDIS data rule out the flavour separation *assumed* for kaons in KRE [18].

In future, very precise data will become available on the production of identified hadrons measured in semi-inclusive DIS by COMPASS and CLAS12 experiments and in pp scattering at RHIC and the LHC.

These new data sets will yield very precise individual parton-to-hadron fragmentation functions derived without assumptions on flavour separation as pioneered by the DSS group. They are an indispensable ingredient for future global QCD analyses of standard PDFs and TMD distributions, the latter are discussed in Section 3.

3 The Transverse Structure of the Nucleon

Modern polarized DIS experiments, capable to also detect and identify hadrons in the final state, are now revealing the intrinsic richness of the nucleon. They aim for exploring two complementary aspects of nucleon structure: the distribution of partons in the transverse plane in momentum space and coordinate space, encoded in the transverse momentum dependent and generalized parton distributions, respectively. These new functions, for the first time, provide a framework for obtaining a three-dimensional picture of the nucleon. The mapping of TMDs and GPDs is a highly complex task that calls for a comprehensive program, combining new dedicated experiments with intense theoretical studies and lattice QCD simulations. The study of these novel parton distributions is a major focus of the CLAS12 physics program. In this chapter we will discuss TMD distribution and fragmentation functions and highlight the particular role strangeness may play.

3.1 Introduction

Parton distribution functions, as introduced in the previous chapter, depend also on the intrinsic parton momentum component k_\perp transverse to that of the nucleon: $f(x, k_\perp)$, so-called transverse momentum dependent distributions (or short TMDs) [20, 21]. The study of TMDs in semi-inclusive DIS was put on a firm theoretical basis with the factorization proof for the kinematic regime where the transverse momentum of the produced hadron is much smaller than the hard scale of the process $P_{hT}^2 \ll Q^2$ [22, 23].

Historically, transverse momentum dependent distribution or fragmentation functions have first been suggested to explain the surprisingly large and otherwise puzzling single-spin asymmetries observed in hadronic reactions with transversely polarized protons.

More recently, TMDs (as well as the GPDs discussed in the next chapter) have received much attention in the context of the so-called 'spin puzzle': the spin of quarks and gluons accounts only for a part of the nucleon spin. A substantial fraction of the nucleon spin must be due to orbital angular momentum. An intriguing aspect of certain TMDs is that nonzero values of these distributions require the presence of nucleon wave function components with different orbital angular momentum. They hence provide information, in a model dependent way, on the elusive parton orbital motion and on spin-orbit effects.

There are eight leading-twist quark TMDs as summarized in Table 1. The three TMDs highlighted in boldface survive integration over k_\perp . These are the unpolarized (polarization averaged) momentum distribution $f_1(x, k_\perp)$ and the helicity distribution $g_1(x, k_\perp)$, discussed in the previous chapter, as well as the transversity distribution $h_1(x, k_\perp)$, which is related to transverse polariza-

N \ q	U	L	T
U	f_1		h_1^\perp
L		g_1	h_{1L}^\perp
T	f_{1T}^\perp	g_{1T}	h_1 h_{1T}^\perp

Table 1: Leading-twist transverse momentum dependent parton distributions. U , L , and T stand for unpolarized, longitudinally polarized, and transversely polarized nucleons (rows) and quarks (columns).

tion of the struck quark. The other five distributions in Table 1 do *not* survive integration over k_{\perp} . They typically describe the correlation between the transverse momentum of quarks, their spin and/or the spin of the nucleon, i.e. spin-orbit correlations.

Three of these TMDs, denoted by the letter h , describe the distribution of transversely polarized partons. In the helicity basis for the spin $\frac{1}{2}$ nucleon, where f_1 and g_1 have their well known probabilistic interpretation, transverse polarization states are given by linear combinations of positive and negative helicity states. Since helicity and chirality are the same at leading twist, the "h" TMDs are therefore called *chiral-odd* distributions. This peculiar property excludes them from influencing any inclusive DIS observable. Chiral-odd TMDs appear in only those observables involving two chiral-odd partners, such as Drell-Yan processes involving two chiral-odd parton distributions or semi-inclusive DIS involving also a chiral-odd fragmentation function.

Two TMDs, the Sivers f_{1T}^{\perp} [24] and the Boer-Mulders h_{1T}^{\perp} [25] distributions, are rather exotic in being naive-time-reversal-odd (short: T-odd)². For a long time T-odd effects were believed to vanish due to time reversal invariance [26]. Recently it was shown that initial and finale-state interactions can produce T-odd effects without violating T-invariance [27, 28, 29]. These T-odd distributions play a crucial role in our understanding of nucleon structure. Their observation, already confirmed for the Sivers distribution, is a clear indication of parton orbital motion and the presence of non-trivial phases from initial or final state interaction, that survive in the Bjorken limit. The origin and expected process dependence of these functions, challenging the traditional concept of factorization and universality of PDFs, are related to fundamental QCD effects. In fact, the symmetry properties of QCD require the Sivers and Boer-Mulders distributions to appear with opposite sign in the expressions for DIS and Drell-Yan cross sections [28]. The experimental verification of this peculiar breaking of universality for T-odd TMD distributions, exhibits an important test for the description of single-spin asymmetries within the framework of QCD. Its invalidation would have profound consequences for our understanding of high-energy reactions involving hadrons. The chiral-even Sivers distribution describes the correlation of the parton intrinsic motion with the nucleon spin, while the chiral-odd Boer-Mulders distribution relates this intrinsic parton motion with its own spin in an *unpolarized* nucleon. Hence, the latter distribution has the striking peculiarity that it might give unexpected spin effects even in unpolarized processes.

Similar correlations arise in the hadronization process. One particular case is the T-odd chiral-odd Collins fragmentation function $H_{1T}^{\perp}(z, P_{\perp})$ [26] representing a correlation between the transverse polarization of the fragmenting quark and the transverse momentum P_{\perp} the produced hadron acquires in the fragmentation process. The Collins function is of high importance for spin physics because it acts as a "quark polarimeter", but it is also interesting on its own because it allows for an exploration of spin and orbital degrees of freedom of the QCD vacuum.

Over the last decade, measurements of azimuthal moments of hadronic cross sections in hard processes have emerged as a powerful tool for probing nucleon structure through transverse single-spin asymmetries. Many experiments worldwide are currently trying to pin down various TMD effects through semi-inclusive DIS (HERMES at DESY [30, 31, 32, 33, 34, 35, 36, 37], COMPASS at CERN [38, 39, 40, 41], CLAS and Hall A at Jefferson Lab [42, 43, 44, 45, 46]) polarized proton-proton collisions (BRAHMS, PHENIX and STAR at RHIC [47, 48, 49, 50, 51, 52, 53, 54, 55, 56]), and electron-positron annihilation (Belle at KEK) [57, 58] and Babar at SLAC [59]).

The JLab 12 GeV upgrade will provide the unique combination of high beam energy, intensity (luminosity) and polarization, the usage of polarized targets and advanced detection capabilities

²Naive time reversal involves the time reversal of three momenta and angular momenta without interchange of initial and final states.

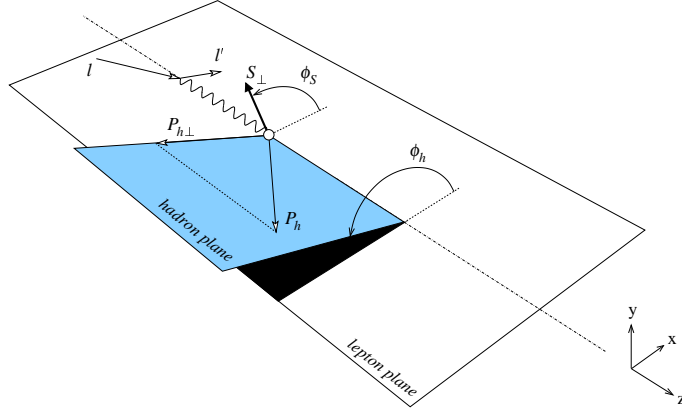


Figure 7: Azimuthal angles in semi-inclusive DIS. For a longitudinally polarized target, $\phi_S=0$ or 180° for negative and positive helicities of the proton, respectively.

necessary to study the transverse momentum and spin correlations in polarized semi-inclusive DIS processes for a variety of hadron species. Full hadron identification over the whole kinematic range will be the key to explore in detail the flavour dependence of TMDs.

3.2 Spin and azimuthal asymmetries in semi-inclusive DIS

When considering the nucleon internal transverse degrees of freedom, new mechanisms emerge that yield to azimuthal asymmetries in the distribution of observed hadrons. Most generally, polarized single-hadron production in semi-inclusive DIS depends on six kinematic variables. In addition to the variables for inclusive DIS, x , y (with $y = (P \cdot q)/(P \cdot l)$), and the azimuthal angle ϕ_S describing the orientation of the target spin vector for transverse polarization, one has three variables for the final state hadron, the longitudinal hadron momentum z_h , the magnitude of transverse hadron momentum P_{hT} , and the azimuthal angle ϕ_h for the orientation of P_{hT} (see also Fig. 3.1).

The semi-inclusive DIS cross section can be written in a model independent way by means of a set of structure functions [21, 60, 61]. At leading twist, this cross section is described by eight such structure functions, which relate to different combinations of the polarization states of the incoming lepton and the target nucleon (for a complete expansion of the structure functions up to twist-3 see Ref. [21]). Largely following the notation of [21], one has

$$\begin{aligned}
\frac{d\sigma}{dx_B dy d\phi_S dz_h d\phi_h dP_{hT}^2} \propto & \left\{ F_{UU,T} + \varepsilon \cos(2\phi_h) F_{UU}^{\cos 2\phi_h} \right. \\
& + S_{\parallel} \varepsilon \sin(2\phi_h) F_{UL}^{\sin 2\phi_h} + S_{\parallel} \lambda_e \sqrt{1 - \varepsilon^2} F_{LL} \\
& + |\mathbf{S}_{\perp}| \left[\sin(\phi_h - \phi_S) F_{UT,T}^{\sin(\phi_h - \phi_S)} + \varepsilon \sin(\phi_h + \phi_S) F_{UT}^{\sin(\phi_h + \phi_S)} \right. \\
& \quad \left. + \varepsilon \sin(3\phi_h - \phi_S) F_{UT}^{\sin(3\phi_h - \phi_S)} \right] \\
& \left. + |\mathbf{S}_{\perp}| \lambda_e \sqrt{1 - \varepsilon^2} \cos(\phi_h - \phi_S) F_{LT}^{\cos(\phi_h - \phi_S)} + \dots \right\}. \quad (4)
\end{aligned}$$

Here, ε is the degree of longitudinal polarization of the virtual photon which can be expressed through y [21], λ_e is the lepton helicity, and S_{\parallel} denotes longitudinal and S_{\perp} transverse target

polarization. The structure functions F_{XY} merely depend on x , z , and P_{hT} . Here, XY refer to the lepton and the nucleon, respectively: U = unpolarized, L, T = longitudinally, transversely polarized. The third subscript $F_{XY,T}$ indicates the contribution from transversely polarized virtual photons.

By choosing specific polarization states and weighting with the appropriate azimuthal dependence, one can extract each structure function in (4). These structure functions contain the information about all eight leading twist quark TMD distributions:

$$F_{UU,T} \sim \sum_q e_q^2 f_1^q \otimes D_1^q \quad F_{LT}^{\cos(\phi_h - \phi_S)} \sim \sum_q e_q^2 g_{1T}^q \otimes D_1^q \quad (5)$$

$$F_{LL} \sim \sum_q e_q^2 g_1^q \otimes D_1^q \quad F_{UT,T}^{\sin(\phi_h - \phi_S)} \sim \sum_q e_q^2 f_{1T}^{\perp q} \otimes D_1^q \quad (6)$$

$$F_{UU}^{\cos(2\phi_h)} \sim \sum_q e_q^2 h_1^{\perp q} \otimes H_1^{\perp q} \quad F_{UT}^{\sin(\phi_h + \phi_S)} \sim \sum_q e_q^2 h_{1T}^q \otimes H_1^{\perp q} \quad (7)$$

$$F_{UL}^{\sin(2\phi_h)} \sim \sum_q e_q^2 h_{1L}^{\perp q} \otimes H_1^{\perp q} \quad F_{UT}^{\sin(3\phi_h - \phi_S)} \sim \sum_q e_q^2 h_{1T}^{\perp q} \otimes H_1^{\perp q}, \quad (8)$$

where e_q is the charge of the struck quark in units of the elementary charge and the symbol \otimes denotes a convolution integral over intrinsic and fragmentation transverse momenta. Here, all distribution and fragmentation functions depend also on the quark transverse momenta before and after scattering k_{\perp} and P_{\perp} , respectively, $f(x, k_{\perp})$ and $F(z, P_{\perp})$, as well as on the scale Q^2 . To date, the transverse momentum dependence of TMDs is still largely unmeasured, and the common assumption of a Gaussian distribution is used in order to resolve the convolution integral. Very little is known about the average intrinsic transverse momentum that defines the Gaussian width, or its flavour and kinematic dependence. In order to pin down such dependences, fully differential measurements of TMD related observables are highly demanded.

Over the last few years, first results on transverse single-spin asymmetries became available from semi-inclusive DIS experiments. Pioneering measurements by the HERMES Collaboration indicated significant azimuthal moments, which, for the first time, relate unambiguously to the Collins ($F_{UT}^{\sin(\phi_h + \phi_S)}$) and Sivers ($F_{UT}^{\sin(\phi_h - \phi_S)}$) effects [36, 37]. As discussed in the following section, striking differences were observed between charged pions and kaons for all TMD observables that are nonzero, indicating a surprisingly significant role sea quarks may play in the transverse structure of the nucleon. Thus measurements with identified strange hadrons over a wide kinematic range will provide the necessary information for clarifying the role of sea quarks and strangeness in particular.

3.2.1 The kaon ‘‘puzzle’’

Figure 8 presents recent HERMES measurements for the Sivers (left) and Collins (right) asymmetries for pions and kaons [36, 37]. A very interesting facet of the data is the magnitude of the K^+ asymmetries, which is nearly twice as large as that of π^+ . As scattering of u quarks dominates these data due to the charge factor, one might naively expect that the K^+ and π^+ asymmetries should be similar. Their difference in size may thus point to a significant role of other quark flavors, e.g. sea quarks. This difference in magnitude for K^+ and π^+ asymmetries is most pronounced for x values around 0.1 and larger, a kinematic region which will be explored in great detail with CLAS12.

Similarly, a very distinct pattern for pion and kaon asymmetries was also found when measuring the azimuthal dependence of the unpolarized cross section, as shown in Fig. 9 [62]. For an

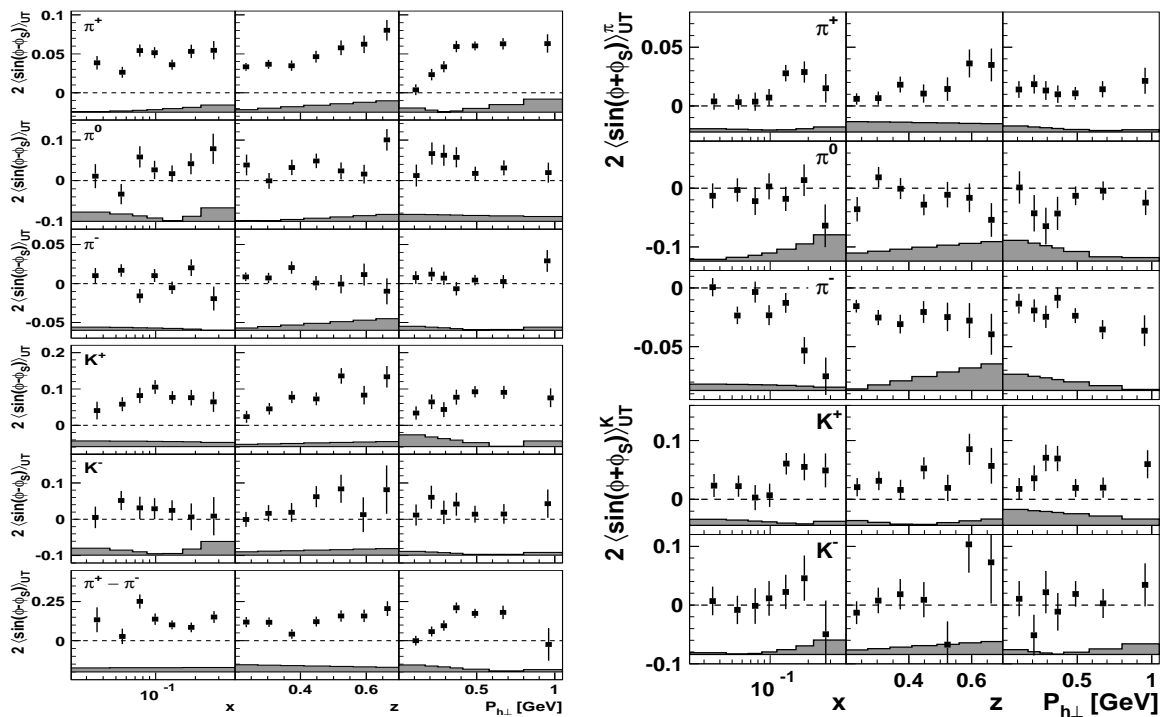


Figure 8: The Siverson (left) and Collins (right) asymmetries for pions and kaons (as indicated in the panels) extracted by the HERMES Collaboration [36, 37].

unpolarized target the only azimuthal asymmetry arising at leading twist is the $\cos 2\phi_h$ modulation in Eq. 4, which relates to the Boer-Mulders distribution h_1^\perp

$$F_{UU}^{\cos 2\phi_h} \propto \sum_q e_q^2 (h_1^{\perp q} \otimes H_1^{\perp q} + \frac{C}{Q^2} f_1^q \otimes D_1^q + \dots) \quad (9)$$

where C is a kinematic factor. The second term in the r.h.s. side of Eq. 9 represents the Cahn effect [63] which contributes at kinematic twist-4 level. In fact, the $\cos \phi_h$ asymmetry shown in the upper row of the panels in Fig. 9 arises from the Cahn effect and the Boer-Mulders function which here both appear at sub-leading twist (twist-3). The Cahn effect accounts for the parton intrinsic transverse momenta in the target nucleon (k_\perp) and the fact that produced hadrons may acquire transverse momenta during the fragmentation process (P_\perp), so that the final hadron transverse momentum P_{hT} is defined as their sum $P_{hT} = zk_\perp + P_\perp$. Theoretical estimates of this effect are still plagued by large uncertainties, mainly related to the insufficient knowledge of the transverse momentum dependence of f_1 and D_1 . Moreover, the average intrinsic transverse momentum k_\perp might depend on the quark flavour; thus a flavour-dependent measure of the Cahn effect in semi-inclusive DIS of identified hadrons is highly desirable.

Looking in more detail at the HERMES measurements presented in Fig. 9, we note, apart from the significantly bigger magnitudes of the K^+ asymmetries, the opposite sign of the $\cos 2\phi$ asymmetry for negative kaons compared to negative pions. This distinct pattern hints at a substantial contribution from sea quarks, in particular from strange quarks. This picture is in agreement with the large magnitude of K^+ amplitudes (larger than the π^+ ones) for the Collins asymmetries $\langle \sin(\phi + \phi_S) \rangle_{UT}$ presented in Fig. 8. Both observations suggest consistently a Collins effect that is larger for kaons than for pions. In particular, the difference with respect to pions can be related

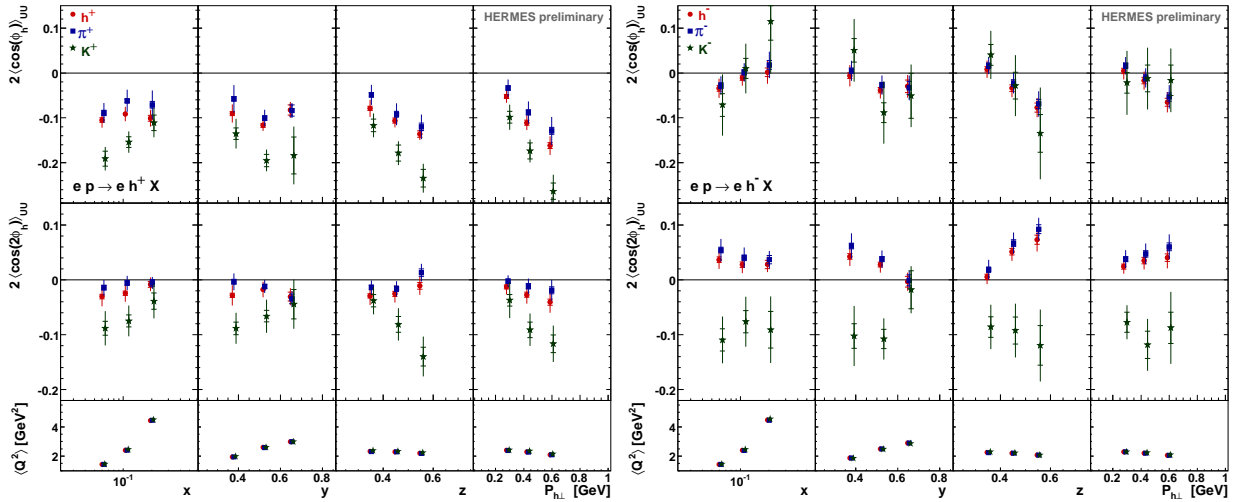


Figure 9: The $\cos \phi$ (upper row of each panel) and $\cos 2\phi$ (lower row of each panel) asymmetries for positively (left) and negatively (right) charged hadrons of different types as indicated in the panels, extracted by the HERMES Collaboration [62].

to a significant contribution of *strange* quark to kaon production.

An extraction of the Boer-Mulders distribution from semi-inclusive DIS is particularly exciting in view of existing measurements of this distribution from Drell-Yan processes [64, 65, 66]: the observed violation of the Lam-Tung relation [67] is a substantial hint for the Boer-Mulders effect [68]. Being a T-odd distribution, just like the Sivers function, the Boer-Mulders function also involves a reversal in sign when going from DIS to Drell-Yan. Experimental verification of this direct prediction of QCD remains outstanding.

3.2.2 Hunting for the Collins function for kaons

The chiral-odd Collins fragmentation function, discussed in the introduction, is an ideal and necessary partner for measuring chiral-odd distributions like transversity and Boer-Mulders distribution in semi-inclusive DIS. This function can be extracted from azimuthal asymmetries in the distribution of back-to-back hadrons in two-jet events in electron-positron annihilation [69]. Pioneering measurements of these asymmetries for pions have been performed by the BELLE Collaboration (KEK) [57, 58]. First global analyses of semi-inclusive DIS and e^+e^- annihilation data yielded recently the milestone extraction [70, 71] of transversity for up and down quarks and the u and d to pion Collins fragmentation functions. They revealed a very peculiar feature of the Collins FF: the *unfavoured* function being of similar magnitude and opposite sign than the *favoured*³ one.

However, no experimental information is available yet about the Collins fragmentation function for *kaons*. Model calculations of the Collins function for kaons [72] indicate that it might be comparable with pion Collins functions. Assuming isospin and charge-conjugation relations, there are in principle seven independent Collins fragmentation functions, but based on the observation that the pion favored Collins function is roughly equal and opposite to the disfavored one, the number of independent Collins functions could be reduced to three. One could then access independent information about the Collins function from semi-inclusive DIS by measuring asymmetries built

³Here, favoured (unfavoured) refers to the case where the fragmenting quark appears (does not appear) as a valence quark in the produced hadron, e.g. the fragmentation of an up quark into a π^+ (π^-).

from the differences between π^+ and π^- and K^+ and K^- using hydrogen and deuterium targets. For example, assuming the strangeness distribution being negligible in the valence kinematic region at sufficiently high values of x , one can built the following ratio:

$$\frac{H_1^{u/K^+} - H_1^{u/K^-}}{H_1^{u/\pi^+} - H_1^{u/\pi^-}} \propto \frac{F_p^{K^+} - F_p^{K^-}}{3(F_p^{\pi^+} - F_p^{\pi^-}) + (F_d^{\pi^+} - F_d^{\pi^-})}, \quad (10)$$

where F_{target}^{hadron} can be any one of four asymmetries related to H_1^\perp , like $\langle \cos 2\phi \rangle_{UU}$, $\langle \sin 2\phi \rangle_{UL}$, $\langle \sin(\phi + \phi_S) \rangle_{UT}$ or $\langle \sin(3\phi - \phi_S) \rangle_{UT}$. Such ratios of asymmetries, simultaneously measured for pions and kaons, will provide independent information about the Collins function for global analyses of TMDs.

3.2.3 Dihadron production in semi-inclusive DIS and transversity

The quark transversity distribution, h_1 , as discussed in the introduction, is one of the three basic quark distributions, together with f_1 and g_1 , that survive k_\perp integration. Experimentally, transversity is quite an elusive object as its chiral-odd nature excludes it from influencing any inclusive observable, which is our main source of information about f_1 and g_1 . It needs to be measured together with another chiral-odd partner. As discussed in previous sections, a very promising way is semi-inclusive DIS involving the chiral-odd transverse momentum dependent Collins fragmentation function in $F_{UT}^{\sin(\phi + \phi_S)}$, as exemplarily presented in Fig. 8 (right).

An interesting, alternative approach is semi-inclusive *dihadron* production from DIS, $ep^\uparrow \rightarrow e'(h_1 h_2)X$, where the two unpolarized hadrons emerge from the fragmentation of the struck quark. The chiral-odd partner of h_1 is represented by the chiral-odd Dihadron Fragmentation Function (DiFF) $H_1^{\not{q}}$ [73, 74]. Such measurements provide complementary information about transversity as here the transverse spin of the fragmenting quark is transferred to the *relative* orbital angular momentum of the hadron pair. Consequently, this mechanism does not require transverse momentum of the hadron pair and standard *collinear* factorization applies.

There is much progress in the field of dihadron fragmentation from both experiment and theory. Very recently, results from pioneering measurements of azimuthal correlations of two pion pairs in back-to-back jets in e^+e^- annihilation related to the dihadron fragmentation function became available from the BELLE Collaboration [75]. On theoretical side, the dihadron cross section was computed up to next-to-leading twist [76] and model calculations for the dihadron fragmentation functions are progressing.

The kinematics of the process is similar to the one in single-hadron semi-inclusive DIS except for the final hadronic state, where now $z = z_{h1} + z_{h2}$ is the fractional energy carried by the hadron pair and the vectors $P_h = P_1 + P_2$ and $R = (P_1 - P_2)/2$ are introduced together with the pair invariant mass M_h , which must be considered much smaller than the hard scale (i.e., $P_h^2 = M_h^2 \ll Q^2$).

Similarly to Eq. 4, the cross section for two-hadron production in semi-inclusive DIS can be expressed by structure functions. When integrating over transverse momenta, only three structure functions appear at leading twist (the full next-to-leading twist expression is given in [76])

$$\frac{d\sigma}{dx_B dy d\phi_R dz d\phi_S dM_h^2 d\cos\theta} \propto \left\{ F_{UU,T} + S_\parallel \lambda_\ell \sqrt{1 - \varepsilon^2} F_{LL} + |S_\perp| \varepsilon \sin(\phi_R + \phi_S) F_{UT}^{\sin(\phi_R + \phi_S)} \right\}, \quad (11)$$

containing the three leading-twist distribution functions f_1, g_1 and h_1 , which now appear in a simple product with the involved fragmentation functions:

$$F_{UU,T} \sim \sum_q e_q^2 f_1^q(x_B) D_1^q(z, \cos \theta, M_h) \quad F_{LL} \sim \sum_q e_q^2 g_1^q(x_B) D_1^q(z, \cos \theta, M_h) \quad (12)$$

$$F_{UT}^{\sin(\phi_R+\phi_S)\sin\theta} \sim \sum_q e_q^2 h_1^q(x_B) H_1^{\curvearrowright q}(z, \cos \theta, M_h). \quad (13)$$

The angle ϕ_R is the azimuthal angle of R_T , the component of R transverse to P_h . A partial wave expansion reveals the structure of the dihadron fragmentation function. For a two-hadron system with low invariant mass $M_h < 1.5$ GeV, dominant contributions come only from the lowest harmonics, i.e., the s and p waves. The expansion in terms of Legendre functions of $\cos \theta$, with the polar angle θ evaluated in the center-of-momentum frame of the hadron pair, yields the factorized expressions

$$D_1 \simeq D_{1,UU} + D_{1,UL}^{sp} \cos \theta + D_{1,LL}^{pp} \frac{1}{4}(3 \cos^2 \theta - 1) \quad (14)$$

$$H_1^{\curvearrowright} \simeq H_{1,UT}^{\curvearrowright sp} + H_{1,LT}^{\curvearrowright pp} \cos \theta. \quad (15)$$

The functions on the r.h.s. depend now only on z and M_h . When applying the symmetrization $f(\theta) + f(\pi - \theta)$, all $\cos \theta$ terms will vanish even if the θ acceptance is not complete but still symmetric about $\theta = \pi/2$. The dominant term is then $H_{1,UT}^{\curvearrowright sp}$, the component of H_1^{\curvearrowright} that is sensitive to the interference between the fragmentation amplitudes into hadron pairs in relative s and p wave states. It allows to study the transversity distribution without the complications of solving convolution integrals over transverse momentum or issues of factorization and evolution. Pioneering measurements of two-pion production from polarized semi-inclusive DIS by HERMES [77, 78] and COMPASS [79, 80, 81] and from e^+e^- annihilation by BELLE [75], provided the necessary information for a first extraction of transversity in the framework of collinear factorization [82].

For a real breakthrough of this promising approach to transversity, much more data over a wide kinematic range are needed. As for all semi-inclusive DIS observables, a safely bias-free extraction is only possible with an analysis that is performed fully differential in all relevant kinematic variables. In the case of polarized dihadron production, the cross section depends on seven kinematic variables, which calls for even higher statistics than in the single hadron production case. Hadron identification over the full accessible momentum range is an essential prerequisite for a full exploration of the flavour dependence of the transversity distribution. Particularly interesting are the KK and $K\pi$ combinations, which exhibit sharp vector resonances, like the ϕ , in the considered low invariant mass range [78]. These channels are ideal tools for studying the sp -wave interference via $H_{1,UT}^{\curvearrowright sp}$, which is the leading part of H_1^{\curvearrowright} giving rise to nonzero observables.

3.3 Spin and azimuthal asymmetries in pp collisions

Historically, the surprisingly large left-right asymmetries measured in hadronic reactions with transversely polarized protons initiated the idea about a transverse momentum dependence of quark distributions in polarized protons. The observation of such asymmetries was frequently quoted as a puzzle or challenge for theory. In fact, for a long time, transverse single-spin asymmetries were assumed to be negligible in hard scattering processes [83]. The work of [24] introduced a transverse momentum dependent quark distribution, now termed the Sivers function, which provides a mechanism for the observed asymmetries that does not vanish at high energies.

The pioneering measurements at FermiLab [84, 85, 86, 87, 88] of these large (up to 0.3-0.4 in magnitude) transverse-spin asymmetries in inclusive forward production of pions in pp collisions $p^\uparrow p \rightarrow \pi + X$, have been greatly confirmed by experiments at RHIC (BNL) at much higher center-of-mass energies of up to $\sqrt{s} = 200$ GeV [53]. A rich variety of single-spin asymmetries for identified hadrons ($\pi^\pm, \pi^0, K^\pm, p, \bar{p}$) measured over a wide kinematic range is now available from the Brahms, Phenix and Star experiments at RHIC [47, 48, 49, 50, 51, 52, 54, 55, 56]. The results exhibit a general pattern: sizable asymmetries are measured at forward-rapidity and for positive Feynman $x_F > 0.3$ which increase in magnitude with increasing x_F and P_{hT} . In contrast, for negative x_F and at mid-rapidity all asymmetries are found to be consistent with zero. Also for the observables in pp reactions, a distinct behaviour for pions, kaons and protons was observed [47].

Several mechanisms have been suggested to explain these asymmetries. At large values of P_{hT} collinear factorization involving twist-3 observables can be applied. An alternative approach using TMDs has been used to describe existing data. Employing recent parameterizations of the Sivers function based on fits to DIS data, a fairly successful description of the observed asymmetries for pion production could be obtained [89].

However, any kind of (standard) TMD factorization for the description of pp reactions failed so far due to the presence of both initial and final state interactions. Only on the basis of precise DIS data, involving a detailed study of the spin- and transverse momentum dependence of hadron production in semi-inclusive DIS, the rich field of results from hadronic collisions might be interpreted within the QCD framework.

4 Nucleon Imaging: GPDs and Exclusive Processes

4.1 Introduction

Complementary information towards a genuine multi-dimensional space and momentum resolution of the nucleon structure is offered by the so-called Generalized Parton Distributions (GPDs) [90, 91, 92]. These new functions, containing the non-perturbative, long distance physics of factorized hard exclusive scattering processes, encompass the familiar PDFs and nucleon form factors as kinematic limits and moments, respectively. GPDs offer opportunities to study a uniquely new aspect of the nucleon substructure: the localization of partons in the plane transverse to the motion of the nucleon. As such they provide a nucleon *tomography*. The ability to describe longitudinal momentum distributions at a fixed transverse localization is a prerequisite for studying the so-called Ji-relation [93], which links a certain combination of GPDs to the total angular momentum of a parton in the nucleon. From this quantity, the still hunted orbital angular momentum of partons in the nucleon could possibly be extracted, a question of crucial importance for an understanding of the nucleon structure.

Measurements of hard exclusive processes, where the nucleon stays intact and the final state is fully observed, are much more challenging than traditional inclusive and semi-inclusive scattering experiments. These exclusive processes require a difficult full reconstruction of final state particles and their cross-sections are usually small, demanding high luminosity machines. Pioneering measurements have been performed at DESY (HERMES, H1 and ZEUS) and JLab (HallA and CLAS). A detailed study of GPDs is one of the central topics of ongoing and near-future experiments at COMPASS and JLab. Most importantly, the JLab 12 GeV upgrade provides the unique combination of high energy, high beam intensity (high luminosity) and advanced detection capabilities necessary for studying low rate exclusive processes.

The exclusive production of real photons, Deeply Virtual Compton Scattering (DVCS), appears to be the theoretically cleanest process for studying GPDs. Similar to inclusive DIS, this process however, does not provide direct flavour dependent information. A flavour *tagging* of GPDs could be gained from hard exclusive production of mesons where the quark content of the meson provides flavour dependent information, similar to semi-inclusive DIS. Moreover, vector meson production provides information about gluon GPDs even in the kinematic regime of JLab12, which predominantly probes the valence quark region: while the exclusive electroproduction of ρ^0 and ω mesons receives contributions from both quark and gluon exchange, the production of ϕ mesons is expected to be dominated by gluon exchange. This unique access to gluon GPDs and hence to the gluon total angular momentum in exclusive ϕ -meson production, underlines the need for kaon identification over the whole kinematic acceptance of CLAS12 also for the measurement of exclusive processes. Kaon identification would significantly enhance also the capabilities for measurements of hard exclusive electroproduction of strangeness.

4.2 Hard exclusive meson production

Generalized parton distributions depend upon four kinematic variables: the Mandelstam variable $t = (p - p')^2$, which is the squared momentum transfer to the target nucleon in the scattering process with p (p') representing the initial (final) four-momentum of the proton; the average fraction x of the nucleon's longitudinal momentum carried by the active parton throughout the scattering process; half the difference in the change of the fraction of the nucleon's longitudinal momentum carried by the active parton at the start and the end of the process, written as the skewness variable ξ ; and the square $-Q^2 = q^2$ of the four-momentum of the virtual photon that

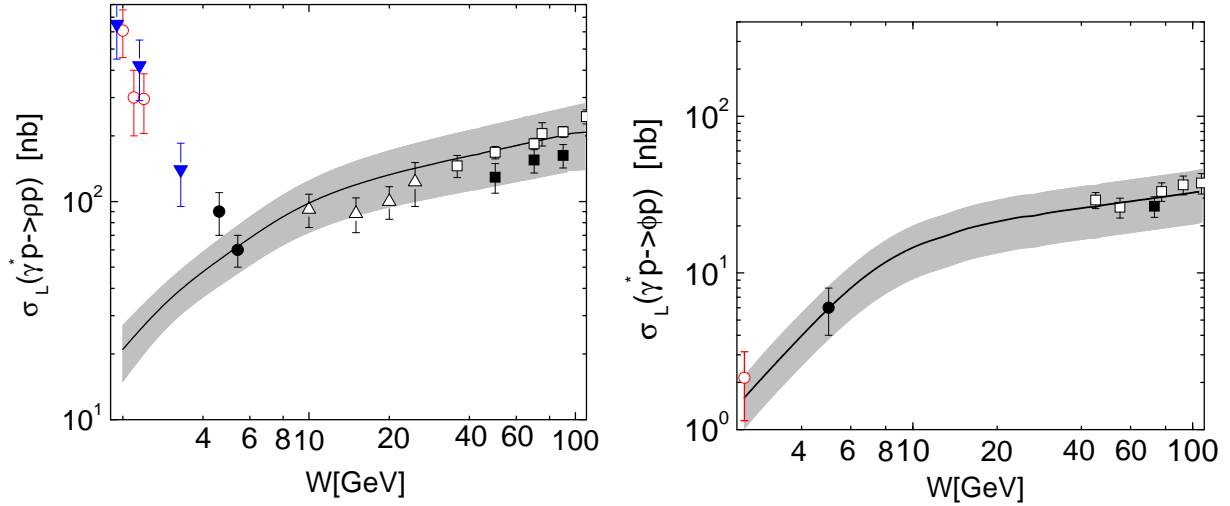


Figure 10: Longitudinal part of the cross section as a function of W , for the exclusive production of ρ^0 (left) and ϕ (right) mesons. The curve is the result of a model calculation from [94, 95, 96] with references for the presented data therein.

mediates the lepton-nucleon scattering process. In the Bjorken limit of $Q^2 \rightarrow \infty$ with fixed t , ξ is related to the Bjorken variable as $\xi \simeq x_B/(2 - x_B)$.

Observables measured in DVCS and hard exclusive meson production provide constraints on GPDs via Compton Form Factors (CFF). Each CFF is a convolution of a hard scattering kernel with a GPD that describes a soft part of the scattering process. For meson production, the meson distribution amplitude enters as a second soft part the factorized cross section. In this case, factorization was proven for longitudinal virtual photons only and an experimental separation of the σ_L and σ_T cross sections is desirable. At high Q^2 , however, the longitudinal part of the cross section is expected to dominate as in this limit $R = \sigma_T/\sigma_L \sim 1/Q^2$. Recent model calculations also take the transverse part of the cross section into account [94, 95, 96] and successfully describe a series of different observables in exclusive meson production. A more recent work emphasizes the very interesting possibility for an access to GPDs for strange quarks from exclusive kaon-hyperon production and highlights the role of transversity GPDs in pseudoscalar meson production [97]. Large, up to 0.4 in magnitude, transverse single-spin asymmetries are predicted for the $K^+\Lambda$ and $K^+\Sigma^0$ channels for the typical kinematics of JLab12. Also for measurements with longitudinally polarized targets or beam, sizeable asymmetries of about 0.05 to 0.1 in magnitude are predicted from the same model calculations [97]. Much progress from theoretical side on GPD model calculations is expected for the near future.

4.2.1 Exclusive ϕ -meson production

Exclusive electroproduction of ϕ mesons provides unique access to the gluon GPD and hence, involving the Ji-relation, to the total angular momentum of gluons. Since the ϕ meson contains mainly strange quarks with a very small admixture of quarks with other flavours, quark-exchange with the nucleon is expected to be suppressed and two- (or more) gluon exchange to dominate. As shown in Fig. 10, available cross section data have been successfully described over a wide range in W , where W is the invariant mass of the photon-nucleon system, using the GPD model

of Ref.s [94, 95, 96]. For the production of ρ^0 mesons, shown in the left panel of Fig. 10, there is a clear indication for a change in the production mechanism around $W = 4$ GeV and the GPD model, where both quark and gluon exchange is taken into account, fails to describe the JLab data at low W . In contrast, ϕ -meson production is well described over two orders of magnitude in W down to values of about 2 GeV by the employed GPD model, which assumes dominance of gluon exchange for this channel. This underlines the usage of exclusive ϕ -meson production as a very suitable channel for studying gluon GPDs and clearly much more data is needed over a wide kinematic range.

Experimentally, ϕ -meson production is a very clean, nearly background free exclusive channel given the kaons from the decay $\phi \rightarrow K^+K^-$ can be identified. A Monte Carlo simulation of the reaction $ep \rightarrow ep\phi, \phi \rightarrow K^+K^-$ obtained with 11 GeV electrons shows that the kaons from the ϕ decay are reaching momenta up to 6 GeV. Hence, kaon identification over the momentum range 1–6 GeV would open the way for detailed measurements of this unique channel for studying the role of gluon GPDs in the valence kinematic region.

5 Hadronization in the Nuclear Medium

5.1 Introduction

An interesting pattern of modifications of parton distribution and fragmentation functions in nuclei has been observed, which caused much excitement and vast experimental and theoretical activities. Generally, the evolution of a fast-moving quark into hadrons is a non-perturbative, dynamic phenomenon and its space-time evolution is a basic issue of physics. The understanding of quark propagation in the nuclear medium is crucial for the interpretation of high energy proton-nucleus interactions and ultra relativistic heavy ion collisions, the latter aiming for studying the Quark-Gluon Plasma. Quark propagation in the nuclear environment involves different processes like multiple interaction with the medium and induced gluon radiation, which lead to attenuation and transverse momentum broadening of hadron yields compared to nucleon targets.

5.2 SIDIS and hadronization in cold nuclear matter

The hadronization process in “free space” has been studied extensively in electron-positron annihilation experiments. As a result, the spectra of particles produced and their kinematic dependences are rather well known (within the limitations discussed in Chapter 2). In contrast, very little is known about the space-time evolution of the process.

Leptoproduction of hadrons has the virtue that the energy and momentum transferred to the hit parton are well determined, as it is “tagged” by the scattered lepton and the nucleus is basically used as a probe at the fermi scale with increasing size or density, thus acting as femtometer-scale detector of the hadronization process. Theoretical models can therefore be calibrated in nuclear semi-inclusive DIS and then applied, for example, to studies of the Quark-Gluon Plasma.

Effects of cold nuclear matter on hadron production in semi-inclusive DIS have been extensively studied by the HERMES experiment at DESY using a 27.6 GeV positron beam on internal gaseous targets of deuterium, helium, neon, krypton or xenon [98]. By using efficient particle identification over the whole kinematic range of the interactions, the measurements have been performed for charged and neutral pions, for charged kaons and for protons and anti-protons, exhibiting very distinct patterns for the different particle types.

The obtained results clearly reveal that the capability of identifying pions, kaons and protons over the whole kinematic range of interest is essential for gaining more insights into the details of the hadronization process. Furthermore, the potential of performing a fully differential analysis is a key to disentangle the various different stages of hadronization.

5.2.1 Nuclear attenuation

The experimental results are usually presented in terms of the hadron multiplicity ratio R_A^h , which represents the ratio of the number of hadrons of type h produced per DIS event on a nuclear target of mass A to that from a deuterium target. Here we only show a few examples that highlight the observed effects. Figure 11 presents the multiplicity ratio R_A^h as a function of the virtual photon energy (ν) for three slices of the fractional virtual photon energy carried by the produced hadron (z). A very striking observation is the behaviour of R_A^h as a function of ν which indicates a clear attenuation at low ν values where the ratio is smaller than one and constantly increases indicating smaller nuclear effects for high energy transferred by the virtual photon. While this behaviour is similar for pions and kaons, it is very different for protons where knock-out processes from the target remnant might contribute to the proton yield. But even for pions and kaons, the

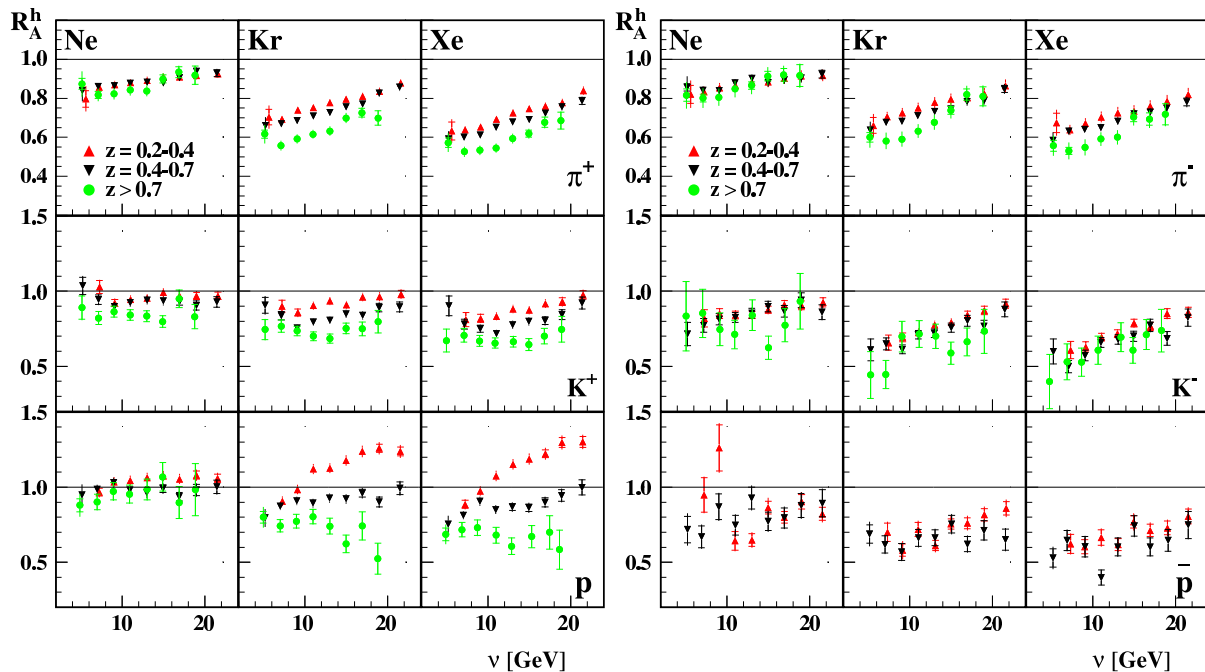


Figure 11: The ν dependence of the multiplicity ratio R_A^h for positively (left) and negatively (right) charged hadrons for three slices in z as indicated in the legend, measured by the HERMES Collaboration [98].

magnitude of attenuation differs for the two hadron types and the different charges. While π^+ and π^- behave very similar, there are clearly visible differences for K^+ and K^- . The various details of attenuation effects become especially pronounced when viewing their multi-dimensional kinematic dependences. Deeper inside into the various different mechanisms causing nuclear effects, would be gained with a fully differential analysis of this observable for identified pions, kaons and protons.

5.2.2 Medium modification of the transverse momentum

A complementary measurement to the hadron attenuation ratio, which is even more sensible to the partonic stage of the hadronization process, is the hadron transverse momentum broadening $\Delta\langle p_t^2 \rangle = \langle p_t^2 \rangle_A^h - \langle p_t^2 \rangle_D^h$. The first direct measurement has been performed by HERMES [99] and is shown in Fig. 12. The panels show the average transverse momentum $\langle p_t^2 \rangle$ for deuterium (top row) and the broadening $\Delta\langle p_t^2 \rangle$ (remaining rows) as a function of either ν , Q^2 , x and z for π^+ or π^- for the various nuclear targets. The data do not reveal a significant dependence on ν while for x and Q^2 the effect slightly increases. In contrast, the effect as function of z shows a clear broadening, which is vanishing as z approaches unity. This indicates both that there is no or little dependence of the primordial transverse momentum on the size of the nucleus and that the p_t -broadening is not due to elastic scattering of pre-hadron or hadrons already produced within the nuclear volume. There is a slight indication for larger p_t -broadening effects for K^+ (bottom panels of Fig. 12) compared to pions but much more statistics is needed to explore a possible hadron type dependence.

The interpretation of this observable would greatly benefit from both a fully differential analysis and full hadron identification. For instance, a multi-dimensional study of the transverse momentum

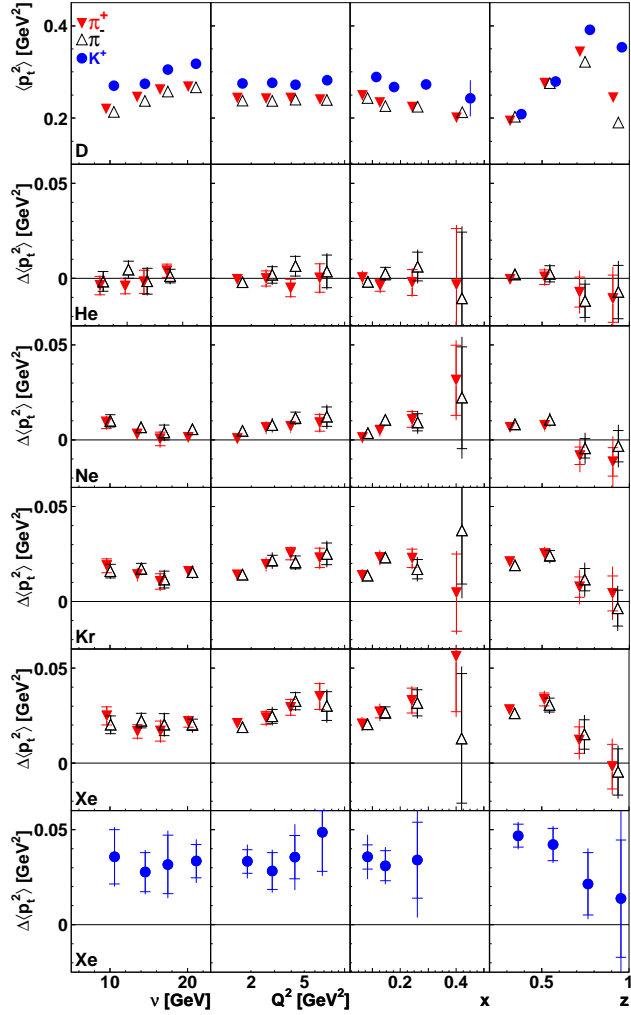


Figure 12: The average transverse momentum $\langle p_t^2 \rangle$ for D (top row) and p_t -broadening $\Delta \langle p_t^2 \rangle$ (remaining rows) for π^+ and π^- produced on He, Ne, Kr, and Xe targets and for K^+ produced on a Xe target (bottom row); measured by the HERMES Collaboration [99].

broadening in nuclear matter, would provide information to distinguish the effects due to the primordial transverse momentum, gluon radiation of the struck quark, the formation and soft multiple interactions of the so-called “pre-hadron” and the interaction of the formed hadrons with the surrounding hadronic medium.

5.2.3 Medium modification of TMD distributions

The study of nuclear effects also opens an alternative way to gain information about certain TMD distributions discussed in Section 3. Azimuthal asymmetries like the $\langle \cos \phi \rangle$ and $\langle \cos 2\phi \rangle$ moments, are expected to be suppressed when being measured in nuclei due to final-state multiple scattering. Model calculations [100] demonstrated a non-trivial transverse momentum dependence of this suppression on the relative shape of the involved TMD quark distributions. Therefore, the nuclear modification of azimuthal asymmetries and the study of its transverse momentum dependence is a very sensitive probe of TMD quark distributions. As shown in Fig. 13 for measurements with a

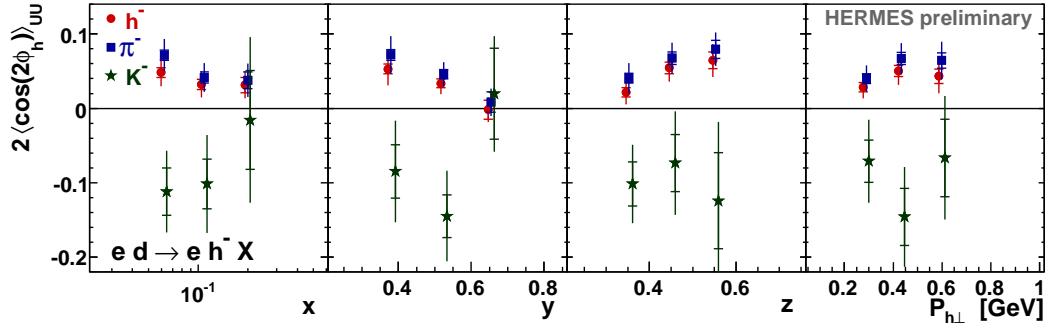


Figure 13: The $\langle \cos 2\phi \rangle$ moments for negatively charged hadrons of types indicated in the figure; extracted by the HERMES Collaboration [62] using a deuterium target.

deuterium target, the shape of the asymmetries for pions and kaons is quite different and hence, nuclear effects are expected to be quite different for the various hadron types. In order to observe such effects, however, measurements with nuclear targets much heavier than deuterium are needed.

6 Spectroscopy: Hidden Strangeness and Strangeonia

The phenomenology of hadrons and in particular the study of their spectrum led more than forty years ago to the development of the quark model, where baryons and mesons are described as bound systems of three quarks and of a quark-antiquark pair, respectively. While this picture still holds and has been proven to reproduce many features of the hadron spectrum, now we know that the hadron mass cannot be explained only in terms of the quark masses, but it is mainly due to the dynamics of the gluons that bind them. Measuring the spectrum of hadrons, studying their properties and inner structure is therefore crucial to achieve a deep knowledge of the strong force.

Mesons, being made by a quark and an anti-quark, are the simplest quark bound system and therefore the ideal benchmark to study the interaction between quarks, understand what the role of gluons is and investigate the origin of confinement. The quark model predicts the existence of multiplets of mesons with similar properties, that are classified according to their total angular momentum J , the parity P , and charge conjugation C . While most of the lowest mass states have been clearly identified and studied [101], several open issues related to the mass hierarchy and decays of excited states remain and still await for a thorough experimental investigation. In addition, phenomenological models [102, 103, 104, 105, 106, 107] and lattice QCD calculations [108, 109] suggest that states beyond the simple $q\bar{q}$ configuration, such as hybrids (qqg), tetraquarks ($qq\bar{q}\bar{q}$) and glueballs, should also exist. If so, we should expect to find a much richer spectrum than that predicted by the quark model and, in particular, we should be able to observe new meson multiplets corresponding to these unconventional configurations. Hybrid mesons are of particular interest as they are the cleanest experimental signature for the presence of gluons in the dynamical mass generation process. A precise determination of their spectrum and properties can provide a unique opportunity to study the role of the glue and to understand the phenomenon of confinement. An unambiguous identification of these states is in general rather difficult, since they can mix with ordinary mesons having the same quantum numbers (J^{PC}). However, the additional degrees of freedom present in these states can also lead to *exotic* quantum numbers that are not allowed in $q\bar{q}$ systems and therefore provide a unique signature of their unusual structure.

MesonEx is an experimental program to study meson spectroscopy via quasi-real photoproduction in Hall B, using the CLAS12 detector and a new Forward Tagger (FT) facility. The 12 GeV electron beam available after the upgrade of Jefferson Laboratory, the excellent characteristics of the CLAS12 detector and the new FT facility will give the possibility of exploring a broad mass range accumulating data of unprecedented accuracy and statistics. As shown in the Sections below, the MesonEx program will greatly benefit from a new RICH detector that will extend the kaon identification capabilities to large momenta of up to 7 GeV.

6.1 Hybrids with hidden strangeness

One very attractive method to identify exotic mesons is through strangeness-rich final states, like the $\phi\pi$ decay mode. Any $s\bar{s}$ -meson decay to $\phi\pi$ is forbidden due to the conservation of isotopic spin. This decay mode is also forbidden for any light $q\bar{q}$ -meson (with q being a u or d quark) by the Okubo-Zweig-Iizuka (OZI) rule. On the other hand, multi-quark or hybrid mesons are expected to have a strong coupling to the $\phi\pi$ system. The discovery of a $\phi\pi$ resonance would indicate a new kind of hadron and suggest a $q\bar{q}g$ or $q\bar{q}q\bar{q}$ state. This is true for $f'\pi$ and $J/\psi\pi$ decay modes as well [110]. Some experimental evidence for the existence of a resonance with strong $\phi\pi$ coupling is available. In experiments at the LEPTON-F spectrometer [111, 112], a new meson $C(1480)$, with mass 1480 ± 40 MeV, width 130 ± 60 MeV and an anomalously large branching ratio to $\phi\pi$, was observed. The angular distributions of the sequential decay $C(1480) \rightarrow \phi\pi^0, \phi \rightarrow K^+K^-$ were studied and

the quantum numbers for $C(1480)$ meson have been determined to be $I^G = 1^+, J^{PC} = 1^{--}$. For this meson, an anomalously large value of the ratio $BR(C(1480) \rightarrow \phi\pi^0)/BR(C(1480) \rightarrow \omega\pi^0) > 0.5$ at 95% C.L. was obtained. This value is more than two orders of magnitude higher than the expected ratio for mesons with the standard isovector quark structure. At present, the only consistent explanation of these properties can be obtained with the assumption that the $C(1480)$ meson is a four quark or hybrid state. At the Ω -spectrometer [113] the cross section for the reaction $\gamma p \rightarrow \phi\pi^0 p$ was measured. Although the number of events was not large (~ 25), an excess of events in the mass spectrum of the $\phi\pi^0$ system at ~ 1.4 GeV was observed. The $\phi\pi^0$ photoproduction cross section was estimated to be $\sigma(\gamma p \rightarrow \phi\pi^0 p) = 6 \pm 3\text{nb}$ (at 95% C.L.). The existence of a structure in the same mass range was confirmed with the study of inclusive $\phi\pi^+$ production with a pion beam [114] and by recent $e^+e^- \rightarrow \phi\pi^0$ data from Ref. [115].

A clean identification of the final state can be obtained by detecting the K^+K^- pair from the charged decay of the ϕ meson. This could be achieved with the CLAS12 base equipment, where a RICH detector that extends kaon identification to momenta beyond 2.5 GeV, would greatly improve the accessible kinematic range for the higher momentum kaons produced in the reaction. Such studies will open a unique window in the search of exotics with hidden strangeness.

6.2 Strangeonia

Strangeonia are mesons containing $s\bar{s}$ pairs: these can be conventional states in the quark model or hybrids with or without exotic quantum numbers. While the strange meson spectrum is quite well understood, the details of the strangeonium spectrum are much less certain and only a handful of states have been confirmed. This, in itself, is a motivation for studying strangeonium spectroscopy. In addition, a number of the final states in which an exotic signal has been claimed are also final states in which strangeonia would be expected. Thus, a precise determination of the strangeonium spectrum is important to constrain the search of exotic candidates.

The masses are expected to be in the 1-3 GeV range, i.e. a transition region between light (relativistic) and heavy (non-relativistic) $q\bar{q}$ states⁴. The conventional *strangeonia* mesons are associated with the radial and orbital excited states of the $\phi(1020)$ meson, the ground state of the $s\bar{s}$ system. Even these "normal" strangeonia are poorly understood: among the 22 low mass ($M < 2.5$ GeV) strangeonium states expected, only 5 are well identified. A summary of the current data on the $\phi(1680)$, i.e. the first radial excitation, is shown in Table 2. The interpretation of the current data is not conclusive. Photoproduction and e^+e^- annihilation experiments observed in fact different properties of the $\phi(1680)$ decay modes than hadroproduction experiments. In addition the resonance mass is systematically higher in photoproduction than in e^+e^- annihilation and there is no evidence of KK^* decay in photoproduction, which on the contrary is found to be dominant in e^+e^- experiments.

The different behavior of the $\phi(1680)$ observed in the two types of experiment may be explained by the presence of two resonances interfering with the light $q\bar{q}$ states. To understand this problem one could measure the relative branching ratios of the $\phi(1680)$ into the neutral and charged KK and KK^* pairs. Another possibility is to study the $\phi\eta$ decay mode since, according to the Zweig rule, the contribution of $s\bar{s}$ states is expected and interference with the light $q\bar{q}$ states should be highly suppressed. Just the mere identification of a resonance in the $\phi\eta$ system will prove the presence of a $s\bar{s}$ state. This argument can be extended to the $\phi(1850)$ and other higher mass

⁴The relevance of this aspect was pointed out by Barnes, Page and Black [116]: "the similarity between the $s\bar{s}$ spectrum, the light meson $q\bar{q}$ and the heavy $Q\bar{Q}$ systems needs to be understood to bridge the gap between Heavy Quark Effective Theory (HQET) and the light quark world in which we live".

<i>production</i>	<i>mass</i> [MeV]	<i>width</i> (MeV)	<i>experiment</i>	<i>decay</i>	ref
e^+e^-	1650		DM1	$K_L K_S$	[117]
	1650			$K^+ K^-$	[118]
	1650		VEPP-2M	$K^+ K^-$	[119]
	1680		DM2	$K^+ K^-$	[120]
	1677	102		$K_S K^+ \pi^-$	[121]
	1680	185	DM1	$KK, KK\pi$	[122]
	1657	146	DM2	$K^+ K^-$	[123]
photo-	1748	80	CERN Omega	KK	[124]
	1760	80	CERN WA57	KK	[125]
	1726	121	Fermi E401	KK	[126]
	1753	122	Fermi FOCUS	KK	[127]

Table 2: Experimental data on the $\phi(1680)$.

excitations. This decay mode has not been yet observed and is one of the main reactions of interest of the MesonEx program. Preliminary analysis of data taken with CLAS are promising, indicating that extraction of strangeonium resonances is feasible. However, due to the limited statistics and energy range, the current data will provide only a partial insight of the strangeonium sector. Higher beam energy together with an extended kaon identification would allow for a much deeper investigation of these states. The present CLAS12 particle identification detectors provide good K/π separation up to momenta of about 2.5 GeV, which corresponds to only a small fraction of the expected momentum range for kaons produced by the decay of strangonia, which extends up to 7 GeV. The addition of a RICH detector would greatly extend the range for measuring kaons, resulting in a dramatic increase of acceptance for the investigation of these meson states and making the upgraded Hall B the ideal place to study strangeonium production.

7 Acknowledgement

We like to thank Y. Amhis, A. Bacchetta, A. Bracco, W. Brooks, V. Burkert, M. Calvetti, E. Christova, A. Courtoy, L. Elouadrhiri, R. Forty, K. Gallmeister, I. Garzia, F. Giordano, S. Gliske, K. Griffioen, K. Hafidi, M. Hoek, T. Iijima, A. Kotzinian, P. Krizan, P. Kroll, F. Kunne, S. Liuti, A. Martin, H. Matevosyan, C. Matteuzzi, S. Melis, F. Murgia, C. Pauly, J. Price, J. Rojo Chacon, A. Rostomyan, S. Stepanyan, I. Strakovsky, O. Teryaev, L. Trentadue, F. Tassarotto, and all participants of the workshop "Probing Strangeness in Hard Processes" (PSHP2010) held in Frascati, Italy in October 2010, for their contribution and very fruitful and stimulating discussions. This workshop was supported by the Argonne National Laboratory, the Laboratory Nazionali di Frascati of the Istituto Nazionale di Fisica Nucleare, the Jefferson Science Associates, the Thomas Jefferson National Accelerator Facility, and the University of Connecticut.

References

- [1] International Workshop on Probing Strangeness in Hard Processes - PSHP2010, <http://www.lnf.infn.it/conference/pshp2010/>.
- [2] The JLab12 Technical Design Report, <http://www.jlab.org/12GeV/>.
- [3] S. Forte, *Acta Phys. Polon.* B41 (2010) 2859, 1011.5247.
- [4] H.L. Lai et al., *JHEP* 04 (2007) 089, hep-ph/0702268.
- [5] R.D. Ball et al., *Nucl. Phys.* B838 (2010) 136, 1002.4407.
- [6] NNPDF, R.D. Ball et al., *Nucl. Phys.* B855 (2012) 153, 1107.2652.
- [7] H.L. Lai et al., *Phys. Rev.* D82 (2010) 074024, 1007.2241.
- [8] A.D. Martin et al., *Eur. Phys. J.* C63 (2009) 189, 0901.0002.
- [9] HERMES, A. Airapetian et al., *Phys. Lett.* B666 (2008) 446, 0803.2993.
- [10] M. Gluck et al., *Phys. Rev.* D63 (2001) 094005, hep-ph/0011215.
- [11] D. de Florian, G.A. Navarro and R. Sassot, *Phys. Rev.* D71 (2005) 094018, hep-ph/0504155.
- [12] G.A. Navarro and R. Sassot, *Phys. Rev.* D74 (2006) 011502, hep-ph/0605266.
- [13] D. de Florian et al., *Phys. Rev. Lett.* 101 (2008) 072001, 0804.0422.
- [14] D. de Florian et al., *Phys. Rev.* D80 (2009) 034030, 0904.3821.
- [15] D. de Florian, R. Sassot and M. Stratmann, *Phys. Rev.* D75 (2007) 114010, hep-ph/0703242.
- [16] COMPASS, M.G. Alekseev et al., *Phys. Lett.* B693 (2010) 227, 1007.4061.
- [17] D. de Florian, R. Sassot and M. Stratmann, *J. Phys. Conf. Ser.* 110 (2008) 022045, 0708.0769.
- [18] S. Kretzer, *Phys. Rev.* D62 (2000) 054001, hep-ph/0003177.
- [19] S. Albino, B.A. Kniehl and G. Kramer, *Nucl. Phys.* B725 (2005) 181, hep-ph/0502188.
- [20] P.J. Mulders and R.D. Tangerman, *Nucl. Phys.* B461 (1996) 197, hep-ph/9510301.
- [21] A. Bacchetta et al., *JHEP* 02 (2007) 093, hep-ph/0611265.
- [22] J.C. Collins and D.E. Soper, *Nucl. Phys.* B193 (1981) 381.
- [23] X. Ji, J. Ma and F. Yuan, *Phys. Rev.* D71 (2005) 034005, hep-ph/0404183.
- [24] D.W. Sivers, *Phys. Rev.* D41 (1990) 83.
- [25] D. Boer and P.J. Mulders, *Phys. Rev.* D57 (1998) 5780, hep-ph/9711485.
- [26] J.C. Collins, *Nucl. Phys.* B396 (1993) 161, hep-ph/9208213.
- [27] S.J. Brodsky, D.S. Hwang and I. Schmidt, *Phys. Lett.* B530 (2002) 99, hep-ph/0201296.

- [28] J.C. Collins, Phys. Lett. B536 (2002) 43, hep-ph/0204004.
- [29] A.V. Belitsky, X. Ji and F. Yuan, Nucl. Phys. B656 (2003) 165, hep-ph/0208038.
- [30] HERMES, A. Airapetian et al., Phys. Rev. Lett. 84 (2000) 4047, hep-ex/9910062.
- [31] HERMES, A. Airapetian et al., Phys. Rev. D64 (2001) 097101, hep-ex/0104005.
- [32] HERMES, A. Airapetian et al., Phys. Lett. B562 (2003) 182, hep-ex/0212039.
- [33] HERMES, A. Airapetian et al., Phys. Rev. Lett. 94 (2005) 012002, hep-ex/0408013.
- [34] HERMES, A. Airapetian et al., Phys. Lett. B622 (2005) 14, hep-ex/0505042.
- [35] HERMES, A. Airapetian et al., Phys. Lett. B648 (2007) 164, hep-ex/0612059.
- [36] HERMES, A. Airapetian et al., Phys. Rev. Lett. 103 (2009) 152002, 0906.3918.
- [37] HERMES, A. Airapetian et al., Phys. Lett. B693 (2010) 11, 1006.4221.
- [38] COMPASS, V.Y. Alexakhin et al., Phys. Rev. Lett. 94 (2005) 202002, hep-ex/0503002.
- [39] COMPASS, M. Alekseev et al., Phys. Lett. B673 (2009) 127, 0802.2160.
- [40] COMPASS, M.G. Alekseev et al., Phys. Lett. B692 (2010) 240, 1005.5609.
- [41] COMPASS, F. Bradamante, (2011), 1111.0869.
- [42] CLAS, H. Avakian et al., Phys. Rev. D69 (2004) 112004, hep-ex/0301005.
- [43] CLAS, H. Avakian et al., AIP Conf. Proc. 792 (2005) 945, nucl-ex/0509032.
- [44] CLAS, M. Osipenko et al., Phys. Rev. D80 (2009) 032004, 0809.1153.
- [45] CLAS, H. Avakian et al., Phys. Rev. Lett. 105 (2010) 262002, 1003.4549.
- [46] CLAS, M. Aghasyan et al., Phys.Lett. B704 (2011) 397, 1106.2293.
- [47] BRAHMS, J.H. Lee and F. Videbaek, (2009), 0908.4551.
- [48] BRAHMS, I. Arsene et al., Phys. Rev. Lett. 101 (2008) 042001, 0801.1078.
- [49] PHENIX, S.S. Adler et al., Phys. Rev. Lett. 95 (2005) 202001, hep-ex/0507073.
- [50] PHENIX, M. Chiu, AIP Conf. Proc. 915 (2007) 539, nucl-ex/0701031.
- [51] PHENIX, A. Adare et al., Phys. Rev. D82 (2010) 112008, 1009.4864.
- [52] PHENIX, V. Dharmawardane, PoS DIS2010 (2010) 222.
- [53] STAR, J. Adams et al., Phys. Rev. Lett. 92 (2004) 171801, hep-ex/0310058.
- [54] STAR, B.I. Abelev et al., Phys. Rev. Lett. 99 (2007) 142003, 0705.4629.
- [55] STAR, B.I. Abelev et al., Phys. Rev. Lett. 101 (2008) 222001, 0801.2990.
- [56] STAR, L.K. Eun, J. Phys. Conf. Ser. 230 (2010) 012041.

- [57] BELLE, K. Abe et al., Phys. Rev. Lett. 96 (2006) 232002, hep-ex/0507063.
- [58] BELLE, R. Seidl et al., Phys. Rev. D78 (2008) 032011, 0805.2975.
- [59] BABAR, I. Garzia, (2012), 1201.4678, Proceedings of Transversity 2011.
- [60] A. Kotzinian, Nucl. Phys. B441 (1995) 234, hep-ph/9412283.
- [61] M. Diehl and S. Sapeta, Eur. Phys. J. C41 (2005) 515, hep-ph/0503023.
- [62] HERMES, F. Giordano and R. Lamb, J.Phys.Conf.Ser. 295 (2011) 012092, 1011.5422.
- [63] R.N. Cahn, Phys. Lett. B78 (1978) 269.
- [64] NA10, S. Falciano et al., Z. Phys. C31 (1986) 513.
- [65] NA10, M. Guanziroli et al., Z. Phys. C37 (1988) 545.
- [66] FNAL-E866/NuSea, L.Y. Zhu et al., Phys. Rev. Lett. 99 (2007) 082301, hep-ex/0609005.
- [67] C.S. Lam and W.K. Tung, Phys. Lett. B80 (1979) 228.
- [68] D. Boer and P.J. Mulders, Nucl. Phys. B569 (2000) 505, hep-ph/9906223.
- [69] D. Boer, R. Jakob and P.J. Mulders, Nucl. Phys. B504 (1997) 345, hep-ph/9702281.
- [70] M. Anselmino et al., Phys.Rev. D75 (2007) 054032, hep-ph/0701006.
- [71] M. Anselmino et al., Nucl. Phys. Proc. Suppl. 191 (2009) 98, 0812.4366.
- [72] A. Bacchetta et al., Phys. Lett. B659 (2008) 234, 0707.3372.
- [73] J.C. Collins, S.F. Heppelmann and G.A. Ladinsky, Nucl. Phys. B420 (1994) 565, hep-ph/9305309.
- [74] A. Bianconi et al., Phys. Rev. D62 (2000) 034008, hep-ph/9907475.
- [75] BELLE, A. Vossen et al., Phys.Rev.Lett. 107 (2011) 072004, 1104.2425.
- [76] A. Bacchetta and M. Radici, Phys. Rev. D69 (2004) 074026, hep-ph/0311173.
- [77] HERMES, A. Airapetian et al., JHEP 06 (2008) 017, 0803.2367.
- [78] S. Gliske, Ph.D. thesis, University of Michigan (2011).
- [79] COMPASS, A. Martin, Czech. J. Phys. 56 (2006) F33, hep-ex/0702002.
- [80] COMPASS, H. Wollny, (2009), 0907.0961.
- [81] COMPASS, C. Braun, To appear in the Transversity 2011 proceedings (2012),
- [82] A. Courtoy, A. Bacchetta and M. Radici, (2011), 1106.5897.
- [83] G.L. Kane, J. Pumplin and W. Repko, Phys. Rev. Lett. 41 (1978) 1689.
- [84] FNAL-E581, D.L. Adams et al., Phys. Lett. B261 (1991) 197.
- [85] FNAL-E581, D.L. Adams et al., Z. Phys. C56 (1992) 181.

- [86] FNAL-E704, D.L. Adams et al., Phys. Lett. B264 (1991) 462.
- [87] FNAL-E704, D.L. Adams et al., Phys. Rev. D53 (1996) 4747.
- [88] FNAL-E704, A. Bravar et al., Phys. Rev. Lett. 77 (1996) 2626.
- [89] U. D'Alesio and F. Murgia, Prog. Part. Nucl. Phys. 61 (2008) 394, 0712.4328.
- [90] D. Mueller et al., Fortsch.Phys. 42 (1994) 101, hep-ph/9812448.
- [91] A. Radyushkin, Phys.Lett. B380 (1996) 417, hep-ph/9604317.
- [92] X.D. Ji, Phys.Rev. D55 (1997) 7114, hep-ph/9609381.
- [93] X.D. Ji, Phys.Rev.Lett. 78 (1997) 610, hep-ph/9603249.
- [94] S. Goloskokov and P. Kroll, Eur.Phys.J. C42 (2005) 281, hep-ph/0501242.
- [95] S. Goloskokov and P. Kroll, Eur.Phys.J. C53 (2008) 367, 0708.3569.
- [96] S. Goloskokov and P. Kroll, Eur.Phys.J. C59 (2009) 809, 0809.4126.
- [97] S. Goloskokov and P. Kroll, Eur.Phys.J. A47 (2011) 112, 1106.4897.
- [98] HERMES, A. Airapetian et al., Eur. Phys. J. A47 (2011) 113, 1107.3496.
- [99] HERMES Collaboration, A. Airapetian et al., Phys.Lett. B684 (2010) 114, 0906.2478.
- [100] J.H. Gao, Z.t. Liang and X.N. Wang, Phys.Rev. C81 (2010) 065211, 1001.3146.
- [101] Particle Data Group, K. Nakamura et al., J. Phys. G37 (2010) 075021.
- [102] R.L. Jaffe and K. Johnson, Phys. Lett. B60 (1976) 201.
- [103] D. Horn and J. Mandula, Phys. Rev. D17 (1978) 898.
- [104] T. Barnes et al., Nucl. Phys. B224 (1983) 241.
- [105] N. Isgur, R. Kokoski and J.E. Paton, Phys. Rev. Lett. 54 (1985) 869.
- [106] N. Isgur and J.E. Paton, Phys. Rev. D31 (1985) 2910.
- [107] P. Guo et al., Phys. Rev. D78 (2008) 056003, 0807.2721.
- [108] J.J. Dudek et al., Phys. Rev. Lett. 103 (2009) 262001, 0909.0200.
- [109] J.J. Dudek et al., Phys. Rev. D82 (2010) 034508, 1004.4930.
- [110] F.E. Close and H.J. Lipkin, Phys. Rev. Lett. 41 (1978) 1263.
- [111] S.I. Bitjukov et al., (2005), physics/0512056.
- [112] S.I. Bitjukov et al., Phys. Lett. 188B (1987) 383.
- [113] OMEGA PHOTON, M. Atkinson et al., Nucl. Phys. B231 (1984) 1.
- [114] Y.M. Antipov et al., Instrum. Exp. Tech. 38 (1995) 581.

- [115] BABAR, B. Aubert et al., Phys. Rev. D78 (2008) 092002, 0807.2408.
- [116] T. Barnes, N. Black and P.R. Page, Phys. Rev. D68 (2003) 054014, nucl-th/0208072.
- [117] F. Mane et al., Phys. Lett. B99 (1981) 261.
- [118] B. Delcourt et al., Phys. Lett. B99 (1981) 257.
- [119] P.M. Ivanov et al., Phys. Lett. B107 (1981) 297.
- [120] DM2, D. Bisello et al., Z. Phys. C39 (1988) 13.
- [121] F. Mane et al., Phys. Lett. B112 (1982) 178.
- [122] J. Buon et al., Phys. Lett. B118 (1982) 221.
- [123] DM2, A. Antonelli et al., Z.Phys. C56 (1992) 15.
- [124] D. Aston et al., Phys. Lett. B104 (1981) 231.
- [125] OMEGA PHOTON, M. Atkinson et al., Z. Phys. C27 (1985) 233.
- [126] J. Busenitz et al., Phys. Rev. D40 (1989) 1.
- [127] FOCUS, J.M. Link et al., Phys. Lett. B545 (2002) 50, hep-ex/0208027.